Int. J. Solids Structures Vol. 29, No. 12, pp. 1463–1498, 1992
Printed in Great Britain.

0020–7683/92 $5.00 + .00

INTERFACIAL FRACTURE IN ELASTIC DIFFUSIVE MEDIA

R. V. CRASTER
Department of Mathematics, Imperial College of Science, Technology and Medicine, London SW7 2BZ, U.K.

and

C. ATKINSON†
Schlumberger Cambridge Research, High Cross, Madingley Road, Cambridge CB3 0EL, U.K.

(*Received* 2 *September* 1991; *in revised form* 7 *November* 1991)

Abstract—Following Atkinson and Craster (*Proc. R. Soc. Lond. A* **434**, 605–633, 1991), Craster and Atkinson (*J. Mech. Phys. Solids*, accepted, 1992), we consider the problem of quasi-static plane strain fracture at the interface between different linear isotropic elastic diffusive solids, i.e. fully coupled poroelastic and thermoelastic materials. The problem of quasi-static growing cracks or the initiation of fracture between the materials is of particular interest. In fabricated materials there is a possibility of imperfect bonding or welding, hence fracture is often initiated near or at the interface. We consider here the slightly simpler case when one of the materials is rigid and the interface is either completely permeable (conducting) or impermeable (insulated). Such an assumption about the interface is common in geophysics and is relevant to the case of two completely different materials welded together in industry.

The solution for impulsively opening cracks is considered here using general potential solutions of the poroelastic (thermoelastic) equations used together with Laplace and Fourier transforms. Solution then proceeds by use of the Wiener–Hopf technique; the resulting transformed results are then examined in the neighbourhood of the crack tip. The oscillatory singularity, as calculated by Williams (*Bull. Seismol. Soc. America* **49**, 199–204, 1959) for interfacial fracture in linear isotropic elasticity, is recovered as a particular case. This oscillatory singularity which predicts interpenetration of the crack walls (England, *ASME J. Appl. Mech.* **32**, 400–402, 1965) need not lead us to disregard the solution, although it invalidates the results on the scale of the contact zone. Provided this zone is much smaller than the crack length, the results are still valid for the zone near the crack tip.

A contact zone model of the Comninou (*ASME J. Appl. Mech.*, 1977) type is then developed. The oscillatory solution is then used as an outer solution in the method of matched asymptotic expansions as in Atkinson (*Int. J. Fracture* **18**, 161–177, 1982a; *Int. J. Fracture* **19**, 131–138, 1982b); this is then matched with an appropriate inner solution to correct for the unphysical interpenetration of the crack walls. This approach is valid for small contact zone lengths due to the interpenetration effect.

The problem of steadily propagating fracture is also briefly considered and the stress intensity factors and distinctive near crack tip pore pressure fields are evaluated.

NOMENCLATURE

α	Biot's coefficient of effective stress, i.e. the ratio of fluid volume to the volume change of solid allowing the fluid to drain, where $0 < \alpha \leqslant 1$
β	is the bulk modulus × the coefficient of thermal expansion
B	Skempton's pore pressure coefficient, (Skempton, 1954) i.e. the ratio of induced pore pressure to the variation of mean normal compression under undrained conditions
c	generalized consolidation coefficient
c_ε	specific heat per unit volume in the absence of deformation
δ_{ij}	Kronecker delta
e	dilatation
ε_{ij}	components of the strain tensor
κ	permeability coefficient
λ_0	coefficient of heat conduction
G	is the shear modulus
$\left.\frac{\mathrm{d}\zeta}{\mathrm{d}p}\right\|_\varepsilon = Q$	is a measure of the change in fluid content generated in a unit reference volume during a change of pressure with the strains kept constant

† Permanent address: Department of Mathematics, Imperial College of Science, Technology and Medicine, London SW7 2BZ, U.K.

m	mass of fluid per unit volume
ν, ν_u	drained and undrained Poisson ratios, where $\nu \leqslant \nu_u \leqslant \frac{1}{2}$
p	pore pressure, i.e. the increase in fluid pressure from a reference pressure p_0
q_i	mass flux vector
ρ_0	reference density
s, ξ	the Laplace and Fourier Transform variables respectively
σ_{ij}	stress tensor
T_0	reference temperature
θ	increase in temperature
u_i	displacement vector
ζ	variation of fluid content per unit reference volume, i.e. mass of fluid per unit volume initial density ρ_0

and the following relations are used in the text:

$$\alpha = \frac{3(\nu_u - \nu)}{B(1-2\nu)(1+\nu_u)} \tag{1}$$

$$Q = \frac{2GB^2(1-2\nu)(1+\nu_u)^2}{9(\nu_u - \nu)(1-2\nu_u)} \tag{2}$$

$$\alpha Q = \frac{2GB(1+\nu_u)}{3(1-2\nu_u)} \tag{3}$$

$$\eta = \frac{1-\nu}{1-2\nu} \tag{4}$$

$$\eta_u = \frac{1-\nu_u}{1-2\nu_u} \tag{5}$$

$$2G_u = \frac{2GB(1+\nu_u)}{3(1-\nu_u)} = \frac{\alpha Q}{\eta_u} \tag{6}$$

$$c = \frac{2\kappa B^2 G(1-\nu)(1+\nu_u)^2}{9(1-\nu_u)(\nu_u - \nu)} \tag{7}$$

$$\tilde{\eta} = \frac{(1-\nu)}{2(\nu_u - \nu)} \frac{Gc}{\kappa(1-\nu_u)(2G_u)^2} \tag{8}$$

For $\nu \leqslant \nu_u \leqslant \frac{1}{2}$ then $\tilde{\eta} \geqslant 1$. Note the saturated, incompressible limit (relevant for soil mechanics) can be recovered by taking $\nu_u \to \frac{1}{2}$, $B \to 1$ with the results that $G_u \to G$, $\tilde{\eta} \to \eta$, $\alpha \to 1$, $c \to 2G_u\kappa$ and $Q \to \infty$.

1. INTRODUCTION

There has been recurrent interest in the problem of interfacial fracture between linear isotropic and anisotropic elastic materials. Bonded materials often fracture at or near the interface (Drory *et al.*, 1988), therefore it is of practical importance to study the mechanism of fracture. By considering the fully coupled linear quasi-static elastic diffusive model of Biot (1941, 1955) we can analyse the effect on fracture of the coupling of the pore pressure or thermal fields (in poroelastic and thermoelastic materials respectively) with stresses applied at infinity. Such materials differ from quasi-static elastic solids as a time dependence is now introduced into the equations, for rapid loadings (compared with the diffusion time scale) the material response is stiffer than for slower loadings. In the rapidly loaded situations the pore fluid (in the poroelastic case) cannot diffuse away rapidly, so the material has a stiffer response. The pore pressure (or temperature) boundary conditions on the surface of the material can affect the response of the material, in particular with impermeable boundaries the fluid can be trapped, or its diffusion hindered, this can affect the response of the material. The quantities of interest, the stress intensity factors or pore pressure (temperature) fields are also time dependent (or in steadily propagating cases, velocity dependent).

To gain a fundamental knowledge of fracture in diffusive elastic materials an understanding of some model problems is required, in particular the singular stress fields and the pore pressure (temperature) fields around a crack tip provide valuable information. In previous works by the authors and others (Rice and Simons, 1976, Rudnicki and Koutsibelas, 1991) some model problems of fractures were considered for homogeneous materials. In Atkinson and Craster (1991) and Craster and Atkinson (1992) impulsively

loaded and steadily propagating fractures were considered for fracture in previously undamaged materials, in some cases this led to situations where the pore pressure boundary conditions on the crack faces were different from those on the fracture plane ahead. The resulting stress intensity factors as functions of time or velocity were then analysed. In a pre-faulted or damaged material, Rice and Simons (1976) and Rudnicki and Koutsibelas (1991) considered the steady propagation of a fracture along a permeable or impermeable interface.

However, in some situations where a pre-existing fault lies at the interface between two different materials, say a saturated highly permeable sandstone overlying an impermeable granite, such homogeneous models are inappropriate and our aim here is to investigate such situations.

The thermoelastic case is of interest in industrial applications and the poroelastic case in geophysics. In particular, geophysicists assume that there are pre-existing faults which are impermeable to the diffusing fluid (Rudnicki and Koutsibelas, 1991) and often fractures or flaws may lie at the interface between different layers of porous material. In industrial situations, cracks at the interface between materials in integrated circuit boards are a cause of circuit failure; this often occurs in an environment where significant heating occurs. There have been to our knowledge no attempts to investigate the interaction between the diffusing species and the solid elastic skeleton in such circumstances.

In linear, isotropic elasticity the oscillatory stress singularity at the crack tip was calculated by Williams (1959) using an eigenfunction approach, but it is usually more convenient to analyse the isotropic elastic bimaterial problem using the analytic function method (Muskhelishvili, 1953). The unphysical interpenetration of the crack walls close to the crack tip was noticed by England (1965) and others. When the two materials are incompressible the oscillatory singularity disappears; in the general case, the oscillatory singularity can be rationalized as the consequence of one of the materials having less tendency to longitudinal expansion. The result is that surface wrinkling of the material occurs, leading to the mathematical result that the materials appear to overlap near the crack tip. The extent of this interpenetration zone varies widely depending on the specific loading; for tensile loading the zone is a small fraction of the crack length. For a shear loading, where the longitudinal expansion is significantly larger and the loading itself acts to close the crack, the zone is consequently a large fraction of the crack length (Willis, 1972).

This interpenetration anomaly was initially thought to invalidate the analysis, the apparent contradiction being rectified by the contact zone model of Comninou (1977, 1978) who formulated the finite length crack problem as a distribution of edge dislocations along the interface with auxiliary conditions. This reduced the problem to solving an integral equation. This model assumes that the crack faces are in contact over a length l (the contact zone), that in addition there is no stress singularity at the inner boundary of the contact region and that the stress is compressive in this contact zone. This last condition was checked by considering the sign of the stress singularity at the crack tip. The resulting equations were then evaluated numerically by Comninou and analytically by Atkinson and Leppington (1983) and later by Gautesen and Dundurs (1987, 1988). In Atkinson (1982a, b) bimaterial problems of semi-infinite and finite length cracks were analysed directly from the governing equations using matched asymptotic expansions and Mellin transform techniques. The small size of the contact zone for tensile fracture and the infinity of solutions for the contact zone length suggest that a numerical method is perhaps not the most accurate method for this problem. That this problem has a unique solution for the largest contact zone length is shown in Shield (1982).

In the analysis by Atkinson (1982a) the Comninou model was analysed and the following conclusions were reached; the oscillatory singularity at the crack tip disappears in the contact zone irrespective of the boundary conditions at the ends of the contact zone, the boundary condition of non-singular normal stress at the beginning of the crack tip zone leads to an equation for the contact zone length with an infinity of solutions. This equation is then evaluated to give the contact zone length consistent with only one contact zone. As the method is independent of particular boundary conditions in the contact zone, alternative

contact zone models (Atkinson, 1977a) can be considered: indeed in Atkinson (1982a) other models are considered and shown to have the same energy release rate as the Comninou model.

Recently there has been renewed interest in interfacial phenomenon with the theory being extended to anisotropic elastic (Qu and Bassani, 1989; Ni and Nemat-Nasser, 1991), elastoplastic (Aravas and Sharma, 1991) and power-law (Champion and Atkinson, 1991) materials. In linear elastic materials the analytical work has mainly centered on the integral equation approach of Gautesen and Dundurs (1987). The theory can also be generalized to dynamic interfacial fracture, e.g. Atkinson (1977b) and more recently Yang *et al.* (1991) for anisotropic dynamic debonding.

The linear theories of isotropic thermoelasticity and poroelasticity were introduced and discussed by Biot (1955, 1941), in particular it is shown there that the two theories in the quasi-static limit are mathematically equivalent. The theories introduce a coupling between the pore fluid (temperature) and the solid elastic skeleton (material). The equations of thermoelasticity are usually uncoupled due to the small coupling parameter (Boley and Wiener, 1960). This is not the case for poroelastic materials and the fully coupled equations need to be solved. Here we wish to consider the effect of both the diffusion of pore fluid (heat) and the presence of an interface. The quasistatic case considered here excludes the existence of dynamic effects and introduces time dependence into the otherwise time-independent elasticity equations through the diffusion process.

The plan of the paper is as follows: we use a technique similar to that of Atkinson and Craster (1991) and Craster and Atkinson (1992) to solve the problem for an impulsively loaded semi-infinite crack between a porous elastic (or fully coupled thermoelastic) half space and a rigid substrate. This solution is in many ways analogous to the "classical" elastic solution in that it predicts interpenetration of the crack faces. The diffusion of pore fluid (or heat in thermoelasticity) results in a time dependent (complex) stress intensity factor. Both permeable and impermeable interfaces are considered; the Comninou contact zone model is then extended to cover these cases using a similar approach to that of Atkinson (1982b).

The analogous steadily propagating fractures are also considered, the stress intensity factors as a function of velocity are derived and concise expressions for the near crack tip pore pressure fields are derived. These fields are driven by the dilatation and as a consequence are oscillatory. This result is of potential use in the verification of the usual assumption that in the fracture of thermoelastic materials the governing equations can be uncoupled.

We follow the notation for porous elastic solids as introduced by Rice and Cleary (1976).

The stress σ_{ij} is given by

$$\sigma_{ij} = 2G\varepsilon_{ij} + \frac{2Gv}{(1-2v)}\delta_{ij}\varepsilon_{kk} - \alpha p\delta_{ij}, \tag{9}$$

and the pore pressure p satisfies the linear relation:

$$p = Q\zeta - \alpha Q\varepsilon_{kk}. \tag{10}$$

The governing equations, where we assume that there are no body forces or fluid sources in the body, are as follows:

(a) The equilibrium equation,

$$\sigma_{ij,j} = 0, \tag{11}$$

(b) Darcy's law, which relates the mass flux to the gradient of the pore pressure, where it is assumed that density fluctuations away from the reference density ρ_0 are small (analogous to the Fourier law of heat conduction for thermoelastic media):

$$q_i = -\rho_0 \kappa p_{,i}, \tag{12}$$

and (c) the mass continuity equation (analogous to the entropy balance equation for thermoelasticity):

$$\frac{\partial m}{\partial t} = -q_{i,i}. \tag{13}$$

Here m is the mass of fluid per unit volume $= \zeta\rho_0$ and ρ_0 is a reference density.

The equations can be written for the thermoelastic case as

$$G\nabla^2 u_i + \frac{G}{(1-2\nu)} e_{,i} - \beta\theta_{,i} = 0, \qquad \lambda_0 \nabla^2\theta = \beta T_0 \frac{\partial e}{\partial t} + c_\varepsilon \frac{\partial \theta}{\partial t}, \tag{14, 15}$$

and for the poroelastic case as

$$G\nabla^2 u_i + \frac{G}{(1-2\nu)} e_{,i} - \alpha p_{,i} = 0, \qquad \frac{\partial p}{\partial t} - \kappa Q \nabla^2 p = -\alpha Q \frac{\partial e}{\partial t}. \tag{16, 17}$$

Both sets of equations have the same structure, the equations are characterized by five independent constants; in the poroelastic case these are G, ν as in an elastic material, ν_u, B to characterize the interaction between solid and fluid constituents and κ which characterizes the permeability of the material and the viscosity of the fluid. Typical values for the material parameters are given in Rice and Cleary (1976), for instance values given there (for Berea Sandstone) are $\nu_u = 0.33$, $\nu = 0.2$, $B = 0.62$, $G = 60$ kbar, c (for water-saturated sandstone) $= 1.6 \times 10^4$ cm s^{-2}, (for Westerly Granite) are $\nu_u = 0.34$, $\nu = 0.25$, $B = 0.85$, $G = 150$ kbar, c (for water-saturated) $= 0.22$ cm s^{-2}. The material properties of rocks vary widely, particularly in their permeabilities. The pore space can, of course, be filled with more viscous oils or gases, hence it is advantageous to keep the theory as general as possible. The following correspondence between the thermoelastic and poroelastic variables can be deduced

$$\alpha \equiv \beta, \quad \frac{1}{Q} \equiv \frac{c_\varepsilon}{T_0}, \quad \kappa \equiv \frac{\lambda_0}{T_0}. \tag{18}$$

If we consider the coupled dilatation–diffusion equations (15) and (17) the coupling occurs through the term $\alpha(\partial e/\partial t)$ (for the sandstone above $\alpha = 0.79$), although for thermoelasticity the coupling can be much weaker, there may be cases where $\partial e/\partial t$ is large, particularly for impulsive loadings, so we retain this term here.

In the case of saturated, incompressible constituents the variation of fluid volume content is equivalent to the dilatation of the material. The equations above now reduce to the simpler set:

$$G\nabla^2 u_i + \frac{G e_{,i}}{(1-2\nu)} - p_{,i} = 0, \qquad \frac{\partial e}{\partial t} = c\nabla^2 e. \tag{19, 20}$$

These are the equations considered in the consolidation problems solved by McNamee and Gibson (1960).

The full poroelastic equations can also be written in terms of ζ, the variation of fluid content per unit volume, where ζ is related to physically more relevant variables by the relation $\zeta = \alpha e + p/Q$; (16) and (17) can now be written as

$$G\nabla^2 u_i + \frac{G}{(1-2\nu_u)} e_{,i} - \alpha Q \zeta_{,i} = 0, \qquad c\nabla^2 \zeta = \frac{\partial \zeta}{\partial t}. \tag{21, 22}$$

Similarly the thermoelastic equations could be written in terms of the entropy. These show that the equations are characterized by the presence of a diffusion equation for the pore fluid and the usual Navier elastic equation with a coupling term. Although (21) and (22) appear superficially to be uncoupled it is important to realize that the boundary conditions are always given in terms of the stress, displacements or pore pressure, the variation of fluid content is not a usual boundary condition. The coupling is therefore just transferred to the boundary conditions.

2. FORMULATION

In order to solve the coupled set of eqns (21) and (22) we introduce a general potential representation which reduces to the McNamee and Gibson (1960) potentials in the soil mechanics limit. Taking the divergence of (21) gives

$$\nabla^2(2G\eta_u e - \alpha Q\zeta) = 0, \tag{23}$$

hence a vector $\underline{\psi}$ can be defined such that

$$\zeta = \frac{2G}{\alpha Q}\left(\frac{-\omega}{2}\nabla\cdot\underline{\psi} + \eta_u e\right), \tag{24}$$

where $\underline{\psi}$ is harmonic and ω is an arbitrary (non-zero) constant. This in turn implies, from (21), that

$$\nabla^2 u_i = e_{,i} - \omega\nabla\cdot\underline{\psi}_{,i}. \tag{25}$$

The notation $,i$ denotes differentiation with respect to x_i. Solutions are given by

$$u_i = \phi_{,i} + (x_k\psi_k)_{,i} + \omega\psi_i. \tag{26}$$

Then (24) implies in general that

$$2G\eta_u\nabla^2\phi + G\left(\frac{\omega + 4(1-\nu_u)}{(1-2\nu_u)}\right)\nabla\cdot\underline{\psi} = \alpha Q\zeta, \qquad \nabla^2\underline{\psi} = 0, \qquad \frac{\partial\zeta}{\partial t} = c\nabla^2\zeta. \tag{27, 28, 29}$$

Choosing $\omega = -4(1-\nu_u)$ reduces the problem to solving the set of equations considered in Biot (1956). The completeness of this representation is shown by Verruijt (1969):

$$\frac{\partial\nabla^2\phi}{\partial t} = c\nabla^4\phi, \qquad \nabla^2\underline{\psi} = 0. \tag{30, 31}$$

For plane strain we take $\underline{\psi} = (0, \psi, 0)$ to get the following expressions for the variables of interest:

$$u_1 = \frac{\partial\phi}{\partial x} + y\frac{\partial\psi}{\partial x}, \quad u_2 = \frac{\partial\phi}{\partial y} + y\frac{\partial\psi}{\partial y} - (3-4\nu_u)\psi, \tag{32}$$

$$\zeta = \frac{G}{G_u}\nabla^2\phi, \qquad e = \nabla^2\phi - 2(1-2\nu_u)\psi_{,y}, \tag{33, 34}$$

$$p = \frac{2G\eta}{\alpha}\nabla^2\phi + 2\alpha Q(1-2\nu_u)\psi_{,y}, \qquad \sigma_{xy} = 2G(\phi_{,xy} + y\psi_{,xy} - (1-2\nu_u)\psi_{,x}), \tag{35, 36}$$

$$\sigma_{xx} = 2G(y\psi_{,xx} - \phi_{,yy} - 2\nu_u\psi_{,y}), \qquad \sigma_{yy} = 2G(y\psi_{,yy} - \phi_{,xx} - 2(1-\nu_u)\psi_{,y}). \tag{37, 38}$$

These representations can be compared to the displacement functions for soil mechanics (the saturated, incompressible limit of the poroelastic theory) derived in McNamee and Gibson (1960). Taking the saturation limit implies that $\zeta = e$ and $v_u \to \frac{1}{2}$ and then by defining

$$\phi = -E \quad \text{and} \quad \underline{\psi} = (0, S, 0), \tag{39}$$

we recover the equations considered there. Note that here we have not used the rock mechanics convention that compressive strains are positive. This convention was adopted by McNamee and Gibson (1960) and the correspondence above is exact when this is taken into account. The McNamee and Gibson potentials were limited to solving normal loading problems, taking the soil mechanics limits before applying the potentials to specific problems limits their use.

The above potentials are identical to the specialized tensile potentials introduced in Atkinson and Craster (1991), if we take

$$\phi = \frac{G_u}{G}\Phi + \Psi \quad \text{and} \quad \psi = \frac{1}{(1-2v_u)}\frac{\partial \Psi}{\partial y}.$$

The advantage of these potentials was the simplified structure on $y = 0$; the restriction was that the undrained shear stress was zero along the x axis. This is the same restriction that applies to the McNamee and Gibson potentials.

To proceed we assume all the field variables are zero for $t < 0$ and Laplace transform the governing equations (30) and (31). We also introduce the following scaling, which scales the Laplace transform variable s out of the governing equations, placing the s dependence in the boundary conditions:

$$X = x\left(\frac{s}{c}\right)^{1/2} \quad \text{and} \quad Y = y\left(\frac{s}{c}\right)^{1/2}, \tag{40}$$

$$\sigma_{ij}(x, y, s) = T_{ij}(X, Y, s)\left(\frac{s}{c}\right)^{1/2}, \quad \zeta(x, y, s) = V(X, Y, s)\left(\frac{s}{c}\right)^{1/2}, \tag{41}$$

$$u_i(x, y, s) = U_i(X, Y, s) \quad \text{and} \quad p(x, y, s) = P(X, Y, s)\left(\frac{s}{c}\right)^{1/2}, \tag{42}$$

$$\phi'(X, Y, s) = \phi(x, y, s)\left(\frac{s}{c}\right)^{1/2} \quad \text{and} \quad \psi'(X, Y, s) = \psi(x, y, s)\left(\frac{s}{c}\right)^{1/2}. \tag{43}$$

The governing equations become

$$\nabla^2_{XY}\psi' = 0, \qquad \nabla^4_{XY}\phi' = \nabla^2_{XY}\phi', \tag{44, 45}$$

here $\nabla^2_{XY} = \dfrac{\partial^2}{\partial X^2} + \dfrac{\partial^2}{\partial Y^2}$. Now, taking the Fourier transform with respect to X, i.e.

$$\bar{\phi}'(\xi, Y, s) = \int_{-\infty}^{+\infty} \phi'(X, Y, s)\, e^{i\xi X}\, dX, \tag{46}$$

gives from (44) and (45) the equations

$$\left(\frac{d^2}{dY^2}-\Gamma^2\right)\left(\frac{d^2}{dY^2}-\xi^2\right)\bar{\phi}'(\xi, Y, s)=0, \qquad \left(\frac{d^2}{dY^2}-\xi^2\right)\bar{\psi}'(\xi, Y, s)=0, \quad (47, 48)$$

where $\Gamma^2=\xi^2+1$.

The solutions to (47) and (48) which decay as $Y\to\infty$ are

$$\bar{\psi}'(\xi, Y, s)=B_1(\xi, s)e^{-|\xi|Y}, \quad \bar{\phi}'(\xi, Y, s)=A_1(\xi, s)e^{-|\xi|Y}+A_2(\xi, s)e^{-\Gamma Y}, \quad (49)$$

we take $|\xi|=\xi_+^{1/2}\xi_-^{1/2}$ with both square roots real and positive for ξ real and positive. The functions $\xi_\pm^{1/2}$ have branch cuts from $i0_\mp$ to $\mp i\infty$. Γ^2 is defined as

$$\Gamma^2=\xi^2+1, \quad (50)$$

Γ, defined to be that branch of the square root with positive real part, can be factorized into a product $\Gamma_+\Gamma_-$ where $\Gamma_\pm=(\xi\pm i)^{1/2}$, i.e. they have branch cuts from $\mp i$ to $\mp i\infty$.

The potentials (49) are then substituted into the potential representations; the constants A_1, A_2, B_1 need to be deduced from the boundary conditions. The transformed representations are given in Appendix 3.

3. PERMEABLE INTERFACE

3.1. *Solution*

For a fracture at the interface between a rigid substrate and a poroelastic material the problem is not symmetric, so we cannot appeal to symmetry to fix some of the boundary conditions. If we take the problem where the interface and the crack faces are permeable then on $y=0$

$$p=0 \ \forall x. \quad (51)$$

Ahead of the crack tip, the materials are bonded together, hence there is no displacement

$$u_1=0 \quad \text{and} \quad u_2=0 \quad \text{for } x>0, \quad (52)$$

and on the crack faces we take an internal loading which may be shear or tensile loading or a combination of both. For mathematical convenience we take the loading to be

$$\sigma_{yy}=-\tau_1 e^{x/a}H(t), \quad \sigma_{xy}=-\tau_2 e^{x/a}H(t) \quad \text{for } x<0, \quad (53)$$

i.e. we are considering a crack loaded with a prescribed internal stress. Physically this corresponds to the difference between an applied far field loading and a resistive stress. Although, clearly, these loadings are idealized, more general loadings can be generated by superposition. The notation τ_1 and τ_2 is used for the crack loadings to indicate mode 1 type tensile loading and mode 2 type shear loading (in homogeneous media) respectively. Due to the inseparability of the problem into purely tensile and shear problems, we expect the near crack tip fields to be characterized by a complex stress intensity factor and the leading singularity to be oscillatory.

Laplace transforming the boundary conditions and scaling as above, the non-zero boundary conditions become

$$T_{YY}=\frac{-\tau_1 c^{1/2}}{s^{3/2}}e^{X/a_1}, \quad T_{XY}=\frac{-\tau_2 c^{1/2}}{s^{3/2}}e^{X/a_1} \quad \text{for } X<0, \quad (54)$$

and $a_1=a(s/c)^{1/2}$ is the scaled value of a. Working in the scaled coordinate system is convenient as the Laplace variable "s" is isolated in a_1, and it is therefore easier to analyse the asymptotic behaviour.

As we have mixed boundary conditions we define the following half-range Fourier transforms. On $Y = 0, X > 0$

$$T_+ = \int_0^\infty T_{YY}(X,0,s)\,e^{i\xi X}\,dX, \qquad \tau_+ = \int_0^\infty T_{XY}(X,0,s)\,e^{i\xi X}\,dX, \tag{55,56}$$

and on $Y = 0, X < 0$

$$U_- = \int_{-\infty}^0 U_1(X,0,s)\,e^{i\xi X}\,dX, \qquad V_- = \int_{-\infty}^0 U_2(X,0,s)\,e^{i\xi X}\,dX, \tag{57,58}$$

and for the pore pressure on $Y = 0$

$$\bar{P} = \int_{-\infty}^\infty P(X,0,s)\,e^{i\xi X}\,dX. \tag{59}$$

Using the above definitions the Fourier and Laplace transformed boundary conditions become:

$$\bar{T}_{YY}(\xi,0,s) = T_+ - \frac{\tau_1 a_1 c^{1/2}}{s^{3/2}(1+i\xi a_1)}, \quad \bar{T}_{XY}(\xi,0,s) = \tau_+ - \frac{\tau_2 a_1 c^{1/2}}{s^{3/2}(1+i\xi a_1)}, \tag{60}$$

and $\bar{U}_1(\xi,0,s) = U_-$, $\bar{U}_2(\xi,0,s) = V_-$, $\bar{P}(\xi,0,s) = 0$.

The notation $\bar{U}_1(\xi, Y, s)$ is used to denote the Fourier transform of $U_1(X, Y, s)$ with respect to X. For the permeable interface we take $\bar{P} = 0$ on the X axis which when used with eqn (A39) gives a direct relation between A_2 and B_1:

$$B_1|\xi| = \bar{\eta}A_2. \tag{61}$$

The displacements and stresses on $Y = 0$ give the following relations between the constants:

$$U_- = -i\xi(A_1 + A_2), \qquad V_- = -|\xi|A_1 - \Gamma A_2 - (3-4\nu_u)B_1, \tag{62,63}$$

$$T_+ - \frac{\tau_1 a_1 c^{1/2}}{s^{3/2}(1+i\xi a_1)} = 2G(\xi^2(A_1+A_2) + 2(1-\nu_u)|\xi|B_1), \tag{64}$$

$$\tau_+ - \frac{\tau_2 a_1 c^{1/2}}{s^{3/2}(1+i\xi a_1)} = 2Gi\xi(A_1|\xi| + \Gamma A_2 + (1-2\nu_u)B_1). \tag{65}$$

The above is a full matrix Wiener–Hopf equation which can be written as:

$$\begin{pmatrix} T_+ \\ \tau_+ \end{pmatrix} - \begin{pmatrix} \dfrac{\tau_1 a_1 c^{1/2}}{s^{3/2}(1+i\xi a_1)} \\ \dfrac{\tau_2 a_1 c^{1/2}}{s^{3/2}(1+i\xi a_1)} \end{pmatrix} = \frac{2G|\xi|}{i\xi\Omega(\xi)} \begin{pmatrix} 2i\xi\bar{\eta}(1-\nu_u) & Z(\xi) \\ -Z(\xi) & 2i\xi\bar{\eta}(1-\nu_u) \end{pmatrix} \begin{pmatrix} V_- \\ U_- \end{pmatrix}, \tag{66}$$

where we have defined $\Omega(\xi)$ and $Z(\xi)$ to be

$$\Omega(\xi) = \xi^2 - (\Gamma|\xi| + (3-4\nu_u)\bar{\eta}), \qquad Z(\xi) = \xi^2(\Gamma - |\xi|) + |\xi|\bar{\eta}(1-2\nu_u). \tag{67,68}$$

By taking the combination $T_+ + i\tau_+$ (or alternatively we could take $T_+ - i\tau_+$) the matrix problem can be reduced to the following functional equation:

$$T_+ + i\tau_+ - \frac{\tau_0 a_1}{(1+i\xi a_1)} = \frac{2G(V_- + iU_-)\xi}{\Omega(\xi)} 2\tilde{\eta}(1-\nu_u) W(\xi). \tag{69}$$

This conveniently reduces the problem to a more standard form; with τ_0 and $W(\xi)$ above defined to be

$$\tau_0 = \frac{c^{1/2}}{s^{3/2}}(\tau_1 + i\tau_2), \qquad W(\xi) = \frac{|\xi|}{\xi} - \left(\frac{1}{2\eta_u} + \frac{1}{2\tilde{\eta}(1-\nu_u)}(\Gamma|\xi| - \xi^2)\right). \tag{70, 71}$$

3.2. *The Wiener–Hopf technique*

In order to utilize the Wiener–Hopf technique, e.g. Noble (1958) we need to arrange the "plus" and "minus" functions in such a way as to have a functional equation which consists of a "minus" function equal to a "plus" function with a common region (or line) of analyticity. First, it is necessary to split the functions $W(\xi)$ and $\Omega(\xi)$ into functions which are analytic and non-zero in the upper and lower complex ξ planes respectively. The functional equation (69) is then split into the standard Wiener–Hopf form: a "plus" function and a "minus" function. When these are equated they are by analytic continuation equal to an analytic function which, in general, is then deduced using the extended form of Liouville's theorem.

The product splits for $W(\xi)$ and $\Omega(\xi)$ are performed in Appendix 1. When these functions are split and the simple pole at i/a_1 is subtracted out, the functional equation (69) becomes

$$\left(T_+ + i\tau_+ - \frac{\tau_0 a_1}{(1+i\xi a_1)}\right)\frac{\Omega_+}{W_+} + \frac{\tau_0 a_1 \Omega_+\left(\frac{i}{a_1}\right)}{W_+\left(\frac{i}{a_1}\right)(1+i\xi a_1)}$$

$$= \frac{(V_- + iU_-)2G\xi 2\tilde{\eta}(1-\nu_u) W_-}{\Omega_-} + \frac{\tau_0 a_1 \Omega_+\left(\frac{i}{a_1}\right)}{(1+i\xi a_1) W_+\left(\frac{i}{a_1}\right)} = \Sigma(\xi), \tag{72}$$

where $\Sigma(\xi)$ is by analytic continuation an analytic function everywhere in the complex ξ plane. The asymptotic behaviour of $W_\pm(\xi)$ and $\Omega_\pm(\xi)$ are required as $|\xi| \to \infty$. From Appendix 1, $W_+ \sim O(\xi_+^{(m+1/2)})$, $W_- \sim O(\xi_-^{-(1/2+m)})$ where $m = (1/2\pi i)\log(3-4\nu)$ and $\Omega_+ \sim 1, \Omega_- \sim -\Omega_0$.

We assume that as $|\xi| \to \infty$, $U_- + iV_- \sim O(\xi_-^{-(n+1/2)})$ which implies that the displacements are $O(r^{n-1/2})$ as $r \to 0$. For non-singular displacements (singular displacements would be unphysical) we require $n > \frac{1}{2}$, hence the stresses are $O(r^{n-3/2})$ and so $T_+ + i\tau_+ \sim O(\xi_+^{-(n-1/2)})$.

In the limit as $|\xi| \to \infty$, using the asymptotic results derived above, it is clear that $\Sigma(\xi)$ is bounded at infinity and tends to zero, and therefore from Liouville's theorem is identically zero everywhere.

We can therefore deduce that

$$T_+ + i\tau_+ \sim \frac{i\tau_0 \Omega_+\left(\frac{i}{a_1}\right)}{W_+\left(\frac{i}{a_1}\right)} \xi_+^{m-1/2}. \tag{73}$$

This gives us the transformed stress intensity factor. The complex power of the transform

(m) is the same as for the elastic problem with drained coefficients. This implies that the fluid diffusion does not alter the nature of the stress singularity. A similar result is found in Atkinson and Craster (1991) and Craster and Atkinson (1992). In the problems considered there the material was homogeneous so the usual square root singularity was recovered; in bimaterial fracture the singularity also depends on the Poisson's ratio. It is to be expected that the drained coefficients appear in m, as the interface is assumed to be permeable so the crack tip is always effectively drained; an identical result occurs in the impermeable case, Section 4.1. If the drained Poisson's ratio $\nu = \frac{1}{2}$ (an incompressible material) the oscillations disappear. However, this case is of little interest here as $\nu \leqslant \nu_u \leqslant \frac{1}{2}$ and so we then recover an incompressible elastic solid.

3.3. *Near crack tip behaviour*

In order to identify correctly the crack tip intensity factors it is necessary to evaluate the stress and pore pressure fields in the neighbourhood of the crack tip.

For the stress fields as $r \to 0$ in the neighbourhood of the crack tip, the stress field is the well known elastic solution. Note here we have a rigid substrate so the usual solution is somewhat simplified. From Williams (1959), the Airy stress function ϕ for the elastic material is given by

$$\phi = \Re e\, r^{\lambda+1}(A\sin(\lambda+1)\theta + B\cos(\lambda+1)\theta + C\sin(\lambda-1)\theta + D\cos(\lambda-1)\theta), \tag{74}$$

for $0 \leqslant \theta \leqslant \pi$ where $\lambda = n + \frac{1}{2} - m$, n integer or $\lambda = n$. A concise method for deducing the constants is given in Hein and Erdogan (1971). Taking $n = -1$, which gives the finite displacements and dominant singular stress field, it can be deduced using the analytic function or Williams (1959) method that

$$\sigma_{yy} + i\sigma_{xy}|_{\theta=0} = \frac{K_1^{(p)}(t) + iK_2^{(p)}(t)}{(2\pi)^{1/2}} r^{i\varepsilon - 1/2}, \tag{75}$$

where

$$\varepsilon = \frac{1}{2\pi}\log(3-4\nu), \tag{76}$$

$K_1^{(p)}(t)$ and $K_2^{(p)}(t)$ are the mode 1 and mode 2 stress intensity factors respectively for the permeable interface; it is convenient to combine them and consider the complex stress intensity factor $K^{(p)}(t) = K_1^{(p)}(t) + iK_2^{(p)}(t)$ which is a function of time due to the diffusion process. The superscript (p) is used to distinguish these stress intensity factors from the impermeable cases [with superscript (im)] derived in Section 5.

Laplace transforming (17) to get

$$s\bar{p} - \kappa Q\nabla^2\bar{p} = -\alpha Q s\bar{e} \tag{77}$$

we can deduce that in the neighbourhood of the crack tip ($r \to 0$) the pore pressure is governed by

$$\nabla^2\bar{p} = 0, \tag{78}$$

which for the permeable interface has to leading order (i.e. as $r \to 0$) the solution

$$\bar{p} = \bar{K}_2^{(p)}(s) r\sin\theta \quad \text{for } 0 \leqslant \theta \leqslant \pi, \tag{79}$$

i.e. a simple eigensolution. The dilatation (to leading order) is

$$e \sim \frac{(1-2\nu)}{2G}(\sigma_{xx}+\sigma_{yy}) = \frac{(1-2\nu)}{G}(\Phi(z)+\Phi^*(z^*)), \tag{80}$$

the * being used to denote the complex conjugate. We therefore find a particular solution of $\kappa\nabla^2\bar{p} = \alpha s\bar{e}$ which satisfies the boundary conditions.

In the above we have used the complex variable notation as in Muskhelishvili (1953)

$$\Phi(z) = e^{-\pi\varepsilon}z^{-1/2-i\varepsilon}\sum_{n=0}^{\infty} a_n z^n, \tag{81}$$

the only term we are interested in here is that with $n = 0$, then taking

$$a_0 = \frac{K^*}{2(2\pi)^{1/2}\cosh(\pi\varepsilon)}, \tag{82}$$

leads to

$$\bar{p} \sim \bar{K}_I^{(p)}(s)r\sin\theta + \frac{(1-2\nu)\alpha s\, e^{\varepsilon(\theta-\pi)}r^{3/2}}{\kappa 2G(2\pi)^{1/2}\cosh(\pi\varepsilon)(1+4\varepsilon^2)}\Re(\bar{K}^{(p)}(s)r^{i\varepsilon}(\tfrac{1}{2}-i\varepsilon)(e^{-3i\theta/2}-e^{i\theta/2})) + \cdots \tag{83}$$

This second term is driven by the dilatation and consequently is also oscillatory. Note also that some care is required in interpreting the above result for the pore pressure. The similarity variable for the diffusion equation is r^2/t and our method is an expansion in small r for t fixed; there is a non-uniform limiting process if the limit as $t \to 0$ is now taken. Such a complication does not arise in the expressions for the stress intensity factors.

It is our aim to find the Laplace transformed stress intensity factors $\bar{K}^{(p)}(s) = \bar{K}_I^{(p)}(s) + i\bar{K}_{II}^{(p)}(s)$, $\bar{K}^{(m)}(s)$ and then invert the Laplace transforms, e.g. (92) and (93) numerically.

4. IMPERMEABLE INTERFACE

4.1. *Solution*

If the interface is now taken to be impermeable, the above analysis can be repeated; the only boundary condition which changes is (51). The boundary condition on the pore pressure becomes

$$\frac{\partial p}{\partial y} = 0 \quad \text{for all } x \text{ on } y = 0. \tag{84}$$

We use the general potential representations derived in Section 2 and the formulae of Appendix 3 to give us directly that

$$\xi^2 B_1 = \Gamma\bar{\eta}A_2. \tag{85}$$

The other equations relating the constants A_1, A_2 and B_1, e.g. (62)–(65) remain unchanged. Solution of the resulting matrix Wiener–Hopf equation follows in an identical fashion leading to the following functional equation

$$\bar{T}_+ + i\bar{\tau}_+ - \frac{\tau_0 a_1}{(1+i\xi a_1)} = \frac{2G(\bar{V}_- + i\bar{U}_-)\xi}{\bar{\Omega}(\xi)}2\bar{\eta}(1-\nu_u)\bar{W}(\xi). \tag{86}$$

We use overbars on the functions to denote those which correspond to the impermeable interface. The functions $\bar{\Omega}(\xi)$ and $\bar{W}(\xi)$ are given by

$$\bar{\Omega}(\xi) = \xi^2 - \frac{|\xi|\xi^2}{\Gamma} + (3-4\nu_u)\bar{\eta} \qquad \bar{W}(\xi) = \frac{|\xi|}{\xi} - \frac{1}{2\eta_u} + \frac{\xi^2(|\xi|-\Gamma)}{2\Gamma\bar{\eta}(1-\nu_u)}. \tag{87,88}$$

The product splits for these functions are sketched in Appendix 1. We can subtract out the simple pole at i/a_1 and using the edge conditions and Liouville's theorem on (86) as before [*cf.* (72)] gives

$$\left(\bar{T}_+ + i\bar{\tau}_+ - \frac{\tau_0 a_1}{(1+i\xi a_1)}\right)\frac{\bar{\Omega}_+}{\bar{W}_+} + \frac{\tau_0 a_1 \bar{\Omega}_+\left(\frac{i}{a_1}\right)}{\bar{W}_+\left(\frac{i}{a_1}\right)(1+i\xi a_1)}$$

$$= \frac{(\bar{V}_- + i\bar{U}_-)2G\xi 2\bar{\eta}(1-\nu_u)\bar{W}_-}{\bar{\Omega}_-} + \frac{\tau_0 a_1 \bar{\Omega}_+\left(\frac{i}{a_1}\right)}{(1+i\xi a_1)\bar{W}_+\left(\frac{i}{a_1}\right)} = 0. \tag{89}$$

Using the asymptotic behaviour of the functions gives the following expression for the near crack tip behaviour of the stress fields

$$\bar{T}_+ + i\bar{\tau}_+ \sim \frac{i\tau_0\bar{\Omega}_+\left(\frac{i}{a_1}\right)}{\bar{W}_+\left(\frac{i}{a_1}\right)}\xi_+^{m-1/2}. \tag{90}$$

The expression is similar to the permeable result (73), the only difference is in the functions $\bar{W}$, $\bar{\Omega}$. In the previous works on diffusive elastic fracture Craster and Atkinson (1992) and Atkinson and Craster (1991) the stress intensity factors for fracture in undamaged materials were found. In the cases where the fracture plane was either completely permeable or impermeable, the only difference in the stress intensity factors was in the split functions, i.e. $N_+(i/a_1)$ replacing $\bar{N}_+(i/a_1)$. The functions N_+ and $\bar{N}_+$ reflected the interaction of the applied stress with the pore pressure boundary condition on the crack faces, hence they also occurred naturally in the mixed pore pressure boundary condition cases. In the cases with permeable/impermeable crack faces ($N_+/\bar{N}_+$ occur) an analogous correspondence may occur in the interfacial mixed pore pressure boundary condition cases. These cases are briefly investigated in Appendix 4.

The near crack tip fields can be evaluated in a similar manner to that in Section 3.3. In the impermeable case the elastic field is once again that identified in Section 3.3. The pore pressure field at the crack tip is governed by $\nabla^2\bar{p} = 0$. The asymptotic behaviour of the pore pressure can thus be identified as

$$\bar{p} \sim p_0(s) + K_3^{(im)}(s) r\cos\theta. \tag{91}$$

5. CRACK TIP FIELDS

Inverting the asymptotic transform results we can match these with the appropriate asymptotic results from Sections 3.3 and 4.2 to identify the intensity factors, e.g. (75). In the neighbourhood of the crack tip we can invert the Fourier transformed stress intensity factors (73) and (90) (i.e. inverting in space) using the Tauberian results in Appendix 2 and recalling the scaling introduced earlier, we find from (75) that the purely Laplace transformed stress intensity factors are given by

$$\bar{K}^{(p)}(s) = (2\pi)^{1/2}(\tau_1 + i\tau_2)\frac{\Omega_+\left(\frac{i}{a_1}\right)a^{(1/2-i\varepsilon)}}{sJ_+\left(\frac{i}{a_1}\right)\gamma(\frac{1}{2}+i\varepsilon)} \tag{92}$$

$$\bar{K}^{(im)}(s) = (2\pi)^{1/2}(\tau_1 + i\tau_2)\frac{\bar{\Omega}_+\left(\frac{i}{a_1}\right)a^{(1/2-i\varepsilon)}}{s\bar{J}_+\left(\frac{i}{a_1}\right)\gamma(\frac{1}{2}+i\varepsilon)}, \tag{93}$$

the superscripts (p) and (im) identifying the permeable and impermeable stress intensity factors respectively. For comparison with previous works on interfacial fracture these results are written in terms of $\varepsilon = \mathrm{im}$; by noting that $\gamma(\frac{1}{2}+i\varepsilon)\gamma(\frac{1}{2}-i\varepsilon) = \pi/\cosh(\pi\varepsilon)$ from Abramowitz and Stegun (1970) these results can be put in a more standard form. The functions $J_+(\xi)$, $\bar{J}_+(\xi)$ are defined in Appendix 1, $\gamma(z)$ is the gamma function as defined in Appendix 2. In particular we can deduce that the complex stress intensity in the elastic case for the loadings we have chosen is given by

$$K^{(e)}(t) = (2\pi)^{1/2}(\tau_1 + i\tau_2)\frac{a^{(1/2-i\varepsilon)}}{\gamma(\frac{1}{2}+i\varepsilon)}H(t). \tag{94}$$

Using a non-dimensional time scale $t' = tc/a^2$ we can invert the Laplace transformed complex stress intensity factors (92), (93) numerically for all times. We take

$$\bar{K}^{(p)}(t') = (2\pi)^{1/2}(\tau_1 + i\tau_2)\frac{a^{1/2-i\varepsilon}}{\gamma(i\varepsilon+\frac{1}{2})}f(t'), \tag{95}$$

with the time dependent scaling factor given by the following inverse Laplace transform,

$$f(t') = \frac{1}{2\pi i}\int_{q-i\infty}^{q+i\infty}\frac{\Omega_+\left(\frac{i}{\sqrt{s}}\right)}{sJ_+\left(\frac{i}{\sqrt{s}}\right)}e^{st'}\,ds \quad \text{for } \Re(q) > 0. \tag{96}$$

Graphs of the real and imaginary parts of $f(t')$ and the modulus (using the non-dimensional time scale $t' = tc/a^2$, for $\nu = 0.2$, $\nu_u = 0.4$) are shown in Figs 1–3 respectively. The graphs also contain the equivalent results for the impermeable case shown as a dashed line; in Figure 3 a small time asymptote is also shown. This small time asymptote is deduced using an heuristic argument based on the energy release rate, see below. The time dependent scaling function (96) and its impermeable analogue contain all the time dependence and illustrate how the classical elastic result is altered by diffusion.

The Laplace inversion (96) is performed numerically using an adaptation of the Talbot (1979) algorithm which is briefly described in Appendix 5. An alternative method is to collapse the inversion integral in Laplace transform space around the branch cut along the negative real axis and evaluate the resulting definite integrals numerically. The two methods produce results which agree to within 1%, although the inversion becomes particularly difficult for short time intervals due to the extremely awkward behaviour of the integrand. In particular the function $J_+(\xi)$ does not tend to a limit independent of the argument of ξ (although it is analytic) as $\xi \to 0$. The behaviour of $J_+(\xi)$ is discussed in some detail in Appendix 1.

For large times $t' \to \infty$, $s \to 0$; using the asymptotic results from Appendix 1 we recover the elastic result suggesting that the long term behaviour is essentially elastic.

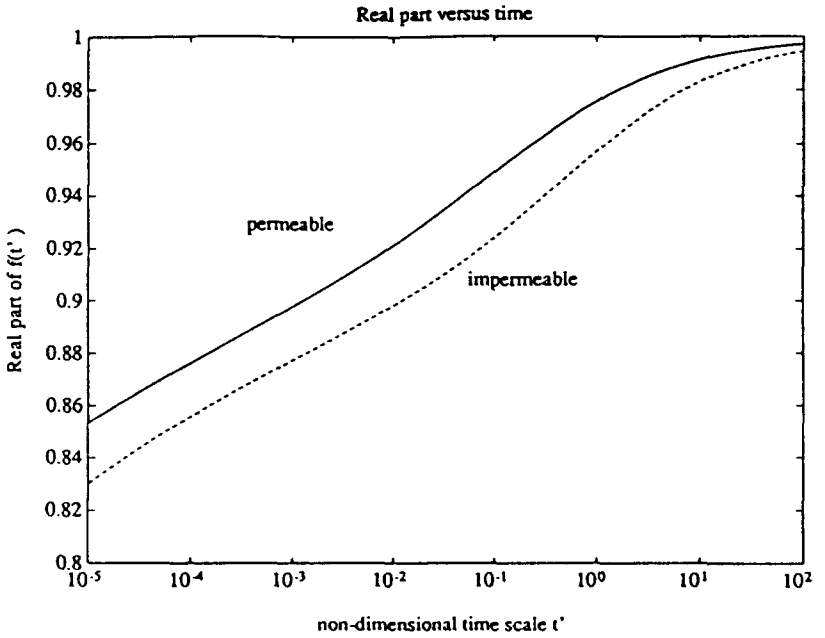

Fig. 1. The real part of the complex scaling factor versus a non-dimensional time scale for $\nu = 0.2$, $\nu_u = 0.4$.

We can check the above results using the same physical argument based on the energy release rate as in Craster and Atkinson (1992), suitably adjusted for the interfacial problem. We visualize the crack tip as a drained elastic inclusion (with Poisson's ratio ν) in an undrained elastic material (with Poisson's ratio ν_u). We can analyse this using the energy release rate. Consider an inclusion with shear modulus μ_i, Poisson's ratio ν_i embedded in a material with shear modulus μ_o, Poisson's ratio ν_o bonded to a rigid substrate, e.g. Fig. 4. Under conditions of plane strain, we define K_i, K_o to be the complex stress intensity factors associated with the inner and outer materials respectively. Then, provided the inclusion is sufficiently small, the energy release rate $\tilde{G}$ is given as

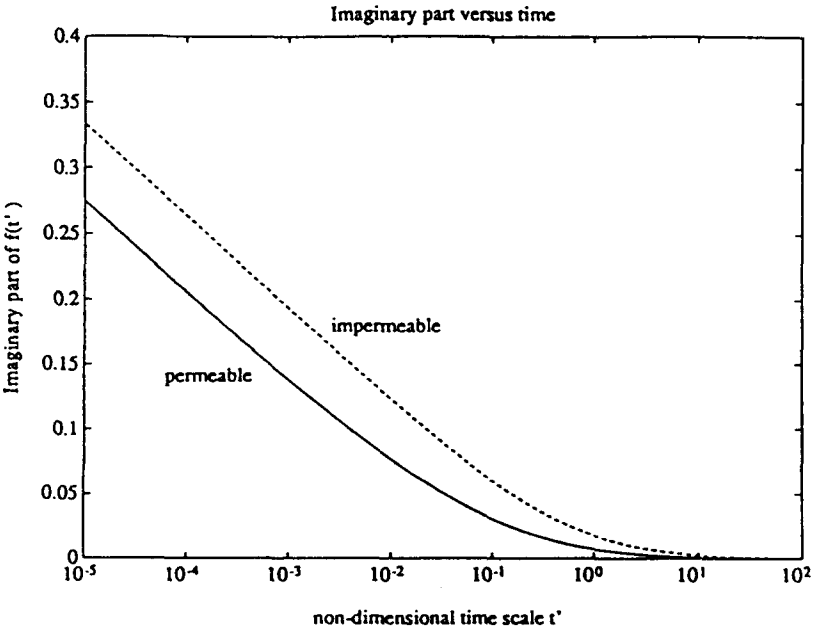

Fig. 2. The imaginary part of the complex scaling factor versus a non-dimensional time scale for $\nu = 0.2$, $\nu_u = 0.4$.

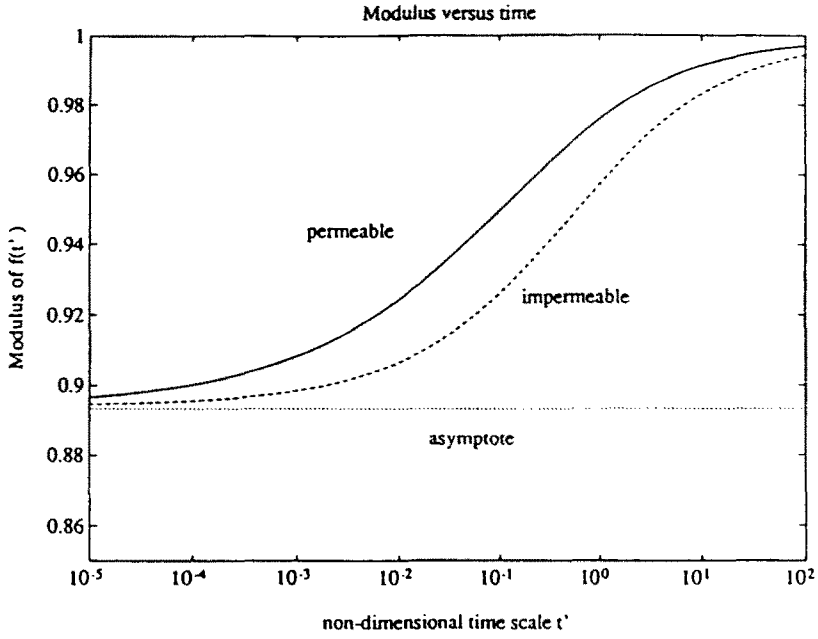

Fig. 3. The modulus of the complex scaling factor versus a non-dimensional time scale for $\nu = 0.2$, $\nu_u = 0.4$.

$$\tilde{G} = \frac{|K_i|^2(1-\nu_i)}{4\mu_i \cosh^2(\pi\varepsilon_i)} = \frac{|K_o|^2(1-\nu_o)}{4\mu_o \cosh^2(\pi\varepsilon_o)}. \tag{97}$$

Here ε_o, ε_i are given by (76) with the outer and inner Poisson's ratios respectively. The energy release rate is calculated as the combination of the work done by the mode 1 and mode 2 stress intensity factors, e.g. Malyshev and Salganik (1965). In physical terms, for small times the local energy release rate at the crack tip must be the same as the energy release rate seen in the far field. We can make this rigorous by using an invariant integral (Atkinson and Craster, 1992). From (97) we find

$$|K_i| = \left(\frac{(3-4\nu_o)(1-\nu_i)}{(3-4\nu_i)(1-\nu_o)}\,\frac{\mu_i}{\mu_o}\right)^{1/2} |K_o|. \tag{98}$$

Letting $\nu_i = \nu$, $\nu_o = \nu_u$, $\mu_i = \mu_o = G$, taking $K_i = K^{(p)}$ or $K^{(im)}$ and

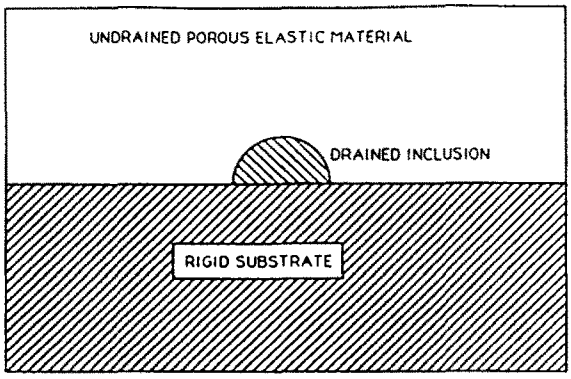

Fig. 4. For short time intervals the crack tip can be visualized as a drained inclusion embedded in an undrained material.

$$K_o = (2\pi)^{1/2}(\tau_1 + i\tau_2)\frac{a^{1/2-i\varepsilon_o}}{\gamma(\frac{1}{2}+i\varepsilon_o)}H(t), \tag{99}$$

we can deduce, for both the permeable and impermeable cases, in the small time limit

$$|f(t')| \to \left(\frac{(3-4\nu_u)(1-\nu)}{(3-4\nu)(1-\nu_u)}\right)^{1/2}\left(\frac{\cosh(\pi\varepsilon_u)}{\cosh(\pi\varepsilon)}\right)^{1/2}H(t'), \tag{100}$$

with $\varepsilon_u = 1/2\pi \log(3-4\nu_u)$. The result (100) was checked against the numerical results and although the small time limit is difficult to evaluate, an extremely good agreement was achieved; this asymptotic result is shown as the straight line in Fig. 3. The energy release rates as functions of t' can also be evaluated from (97)

$$G^{(im)}(t') = \frac{|K^{(im)}(t')|^2(1-\nu)}{4G\cosh^2(\pi\varepsilon)} \tag{101}$$

these are shown (normalized by dividing through by the elastic energy release rate for a homogeneous elastic solid, i.e. $G_e = 2|(\tau_1+i\tau_2)|^2 a(1-\nu)/4G$) in Fig. 5. Also shown there for comparison are the normalized energy release rates for the homogeneous (unmixed) cases using the stress intensity factors given in eqns (85), (88) of Craster and Atkinson (1992). As $t' \to 0$ the curves for the impermeable and permeable cases tend to the same limit, this is because in the unmixed cases the small time limit for the stress intensity factors are identical. This can be shown by considering the inclusion argument above. It can be clearly seen that for the values we have taken ($\nu = 0.2$, $\nu_u = 0.4$), the interfacial energy release rate results for both permeable and impermeable interfaces are, for most time intervals less than the equivalent result for the homogeneous material. For very small t' the situation reverses with more energy release rate for the interfacial cases, in this limit the differences are small.

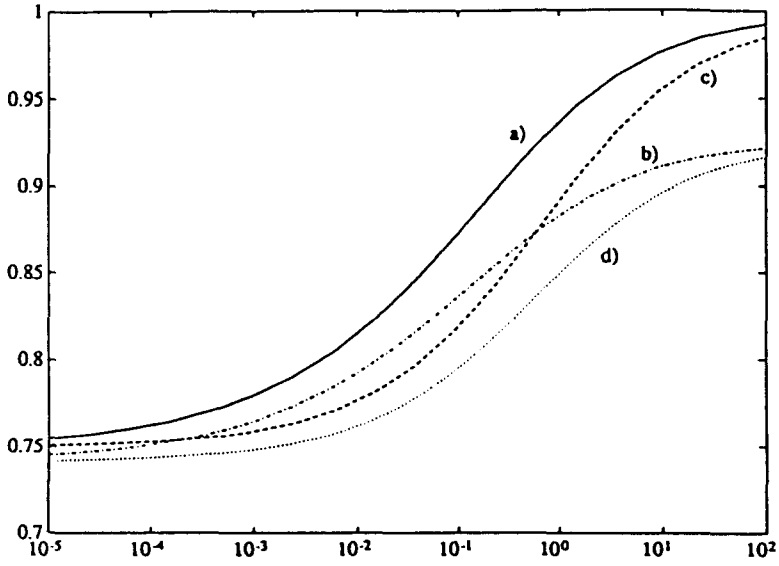

Fig. 5. The energy release rates (normalized as in the text) as functions of $t' = tc/a^2$ for Poisson's ratios $\nu = 0.2$, $\nu_u = 0.4$ the curves correspond to (a) the permeable homogeneous, (b) the permeable interfacial, (c) the impermeable homogeneous and (d) the impermeable interfacial cases respectively.

6. CONTACT ZONE

We now proceed to consider a Comninou (1977) contact zone model. In this section we will deal with the permeable interface only; the impermeable results can be deduced in a similar manner. The contact zone model corrects for the interpenetration of the crack faces; the analysis follows the analytical approach for linear elastic interfacial fracture of Atkinson (1982a,b).

Note we here work entirely in the Laplace transform domain, thereby removing the time dependence explicitly from the equations.

Considering the near crack tip displacement fields, for the permeable case we can invert the asymptotic result for the displacements from (72) to get

$$\bar{u}_2 + \mathrm{i}\bar{u}_1|_{\theta=\pi} = \frac{(\tau_1 + \mathrm{i}\tau_2)}{s} \frac{\Omega_+\left(\frac{\mathrm{i}}{a_1}\right)}{J_+\left(\frac{\mathrm{i}}{a_1}\right)} \frac{(3-4\nu)}{2G} \frac{e^{-\pi\varepsilon}(-x)^{(1/2+\mathrm{i}\varepsilon)} H(-x) a^{1/2-\mathrm{i}\varepsilon}}{(\frac{1}{2}+\mathrm{i}\varepsilon)\gamma(\frac{1}{2}+\mathrm{i}\varepsilon)}. \tag{102}$$

This reduces to the elastic case in the appropriate limits. We find the usual situation for interfacial fracture, the jump in normal displacement across the crack changes sign infinitely often leading to the non-physical interpenetration of the crack faces. Comninou (1977) suggests that this can be corrected by assuming that the crack faces remain in contact over this region.

We let l_1 denote the length of the contact zone, and use polar coordinates centered on the crack tip, with $\theta = 0$ being the line ahead of the crack, i.e. Fig. 6. Then the boundary conditions become, (where we remind the reader that $\bar{u}_2 = \bar{u}_\theta \cos\theta$ on $\theta = 0, \pi$) on $\theta = \pi$:

$$\bar{u}_\theta = 0 \quad \text{for } 0 < r < l_1, \qquad \bar{\sigma}_{\theta\theta} = -\frac{\tau_1}{s} e^{-r/a} \quad \text{for } l_1 < r < \infty, \tag{103, 104}$$

$$\bar{\sigma}_{r\theta} = -\frac{\tau_2}{s} e^{-r/a} \quad \text{for } 0 < r < \infty, \tag{105}$$

and on $\theta = 0$ the same conditions as before (Section 3.1),

$$\bar{u}_r = \bar{u}_\theta = 0, \tag{106}$$

and on $\theta = 0$ and π, for the permeable interface, $\bar{p} = 0$.

The length scale of the loading, a, is assumed greater than the contact zone length, l_1. This length, l_1, for the elastic problem is determined in Comninou (1977) by determining the loading length scale a such that $\sigma_{\theta\theta}|_{\theta=\pi}$ has no stress singularity at the inner boundary of the contact region and is compressive for $0 < l_1 < a$. The contact zone length for

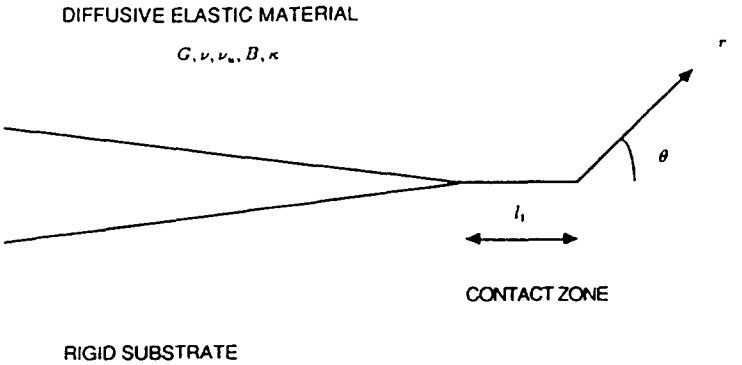

Fig. 6. The coordinate system for the contact zone.

particular materials is determined in an inverse manner; the length is specified and then the ratios that the elastic constants must have is calculated.

These conditions are not assumed *a priori* here [or in Atkinson (1982a, b)]. This is a considerable advantage over the numerical methods.

Now let the solution found earlier in our Wiener–Hopf analysis be the outer solution [which we shall denote using a superscript (o)]. This will be valid for distances δ much greater than l_1, the contact zone length, from the crack tip at $r = 0$. This earlier "outer" solution is clearly non-physical close to the crack due to the interpenetrating property previously referred to. Therefore we need to correct for this behaviour. We recall here that in this section we are dealing with the permeable case. To proceed we write

$$\bar{u}_i = \bar{u}_i^{(i)} + \bar{u}_i^{(o)}, \quad \bar{\sigma}_{ij} = \bar{\sigma}_{ij}^{(i)} + \bar{\sigma}_{ij}^{(o)}, \quad \bar{p} = \bar{p}^{(i)} + \bar{p}^{(0)}, \tag{107}$$

where these outer solutions (o) are the solutions to the problem posed in Section 3.1. The boundary conditions for the "inner" problem [denoted by a superscript (i)] become on $\theta = \pi$:

$$\bar{u}_\theta^{(i)} = -\bar{u}_\theta^{(o)} \quad \text{for } 0 < r < l_1, \qquad \bar{\sigma}_{\theta\theta}^{(i)} = 0 \quad \text{for } l_1 < r < \infty, \qquad \bar{\sigma}_{r\theta}^{(i)} = 0 \quad \text{for } 0 < r < \infty. \tag{108, 109, 110}$$

Defining new coordinates (R, θ) by

$$r = l_1 R, \quad \theta = \theta, \tag{111}$$

i.e. scaling on the length scale of the contact zone we therefore rescale the displacement, stress and pore pressure fields according to

$$\bar{u}_i^{(i)} = l_1^{1/2} \bar{U}_i, \quad \bar{\sigma}_{ij}^{(i)} = l_1^{-1/2} \bar{T}_{ij}, \quad \bar{p}^{(i)} = l_1^{-1/2} \bar{P}. \tag{112}$$

The Laplace transformed diffusion equation becomes

$$s\bar{P} - s\alpha Q \bar{U}_{i,i} = \frac{\kappa Q}{l_1^2} \nabla^2 \bar{P}, \tag{113}$$

where the differentiation is now with respect to (R, θ). In the limit as $l_1 \to 0$ the pore pressure separates out from the dilatation. Hence the governing equations become

$$\nabla^2 \bar{P} = 0 \qquad G\nabla^2 \bar{U}_i + \frac{G}{(1-2\nu)} \bar{E}_{,i} - \alpha \bar{P}_{,i} = 0. \tag{114, 115}$$

From the asymptotic behaviour of the pore pressure (Section 3.3); $\bar{P} \sim \bar{K}_2^{(P)}(s) R l_1^{3/2} \sin\theta$. Therefore to leading order the pore pressure is zero. Hence the situation is analogous to that considered in Atkinson (1982a, b) therefore we just sketch the solution here.

Applying this change of variable (111) and the scalings (112) we can deduce that on $\theta = \pi$

$$\bar{U}_\theta = l_1^{-1/2} \bar{u}_2^{(o)} \quad \text{for } 0 < R < 1, \qquad \bar{T}_{\theta\theta} = 0 \quad \text{for } 1 < R < \infty, \tag{116, 117}$$

$$\bar{T}_{R\theta} = 0 \quad \text{for } 0 < R < \infty, \tag{118}$$

and on $\theta = 0$

$$\bar{U}_\theta = \bar{U}_R = 0. \tag{119}$$

From (102)

$$l_1^{-1/2}\bar{u}_2^{(0)} = \Re\left(\frac{(\tau_1+i\tau_2)}{s}\frac{\Omega_+\left(\frac{i}{a_1}\right)}{J_+\left(\frac{i}{a_1}\right)}\frac{(3-4\nu)}{2G}\frac{e^{-\pi\varepsilon}\left(\frac{-Xl_1}{a}\right)^{i\varepsilon}(-Xa)^{1/2}}{(\frac{1}{2}+i\varepsilon)\gamma(\frac{1}{2}+i\varepsilon)}\right). \tag{120}$$

The scaled displacements satisfy, to leading order, the governing equation

$$G\nabla^2\bar{U}_i + \frac{G}{(1-2\nu)}\bar{E}_{,i} = 0. \tag{121}$$

One natural method for solving bimaterial problems is to use the Mellin transform for the full poroelastic equations. This would lead to a differential difference equation and so it is easier, for the full problem, to use the Fourier transform as in Section 3.1. However, on the scale of the contact zone, the pore pressure equation separates (to leading order) and we are left with the usual Navier equation (with drained Poisson's ratio). We now solve this problem using the Mellin transform which is defined as

$$\Lambda(q) = M(\lambda, q) = \int_0^\infty \lambda(R)R^{q-1}\,dR, \tag{122}$$

and the inversion formula

$$\lambda(R) = \frac{1}{2\pi i}\int_{c-i\infty}^{c+i\infty}\Lambda(q)R^{-q}\,dq, \tag{123}$$

where c is chosen such that $R^{c-1}\lambda(r)$ is absolutely integrable on $(0, \infty)$. We proceed by defining the following transforms (which are unknown functions of q):

$$M(R^2\bar{T}_{00})|_{\theta=\pi} = \bar{F}_- = \int_0^1 R^{q+1}\bar{T}_{00}(R,0)\,dR. \tag{124}$$

This function is analytic in some right half plane for $\Re(q) > q_1$ where q_1 depends on the nature of $\bar{T}_{00}$ as $R \to 0$ and

$$M\left(R^2\frac{\partial\bar{U}_\theta}{\partial R}\right)\Big|_{\theta=\pi} = \bar{G}_- = \int_1^\infty R^{q+1}\left(\frac{\partial\bar{U}_\theta}{\partial R}\right)dR, \tag{125}$$

which is analytic in some left half plane for $\Re(q) < q_0$ where q_0 depends on the behaviour of $\partial\bar{U}_\theta/\partial R$ as $R \to \infty$. The following functional equation can be deduced

$$T(q)\left(G_-(q) + \frac{1}{2}\left(\frac{E}{(q+\frac{1}{2}+i\varepsilon)} + \frac{E^*}{(q+\frac{1}{2}-i\varepsilon)}\right)\right) = -F_+(q), \tag{126}$$

with the * denoting the complex conjugate and

$$T(q) = \frac{G\left(\cos(2q\pi) + \frac{(1+(3-4\nu)^2)}{2(3-4\nu)}\right)}{(1-\nu)\sin(2q\pi)} \tag{127}$$

This is identical to the functional equation deduced in Atkinson (1982a, b) with appropriate

changes made for the rigid boundary and the particular loading considered here and E in (126) defined as

$$E = \frac{(\tau_1 + i\tau_2)}{s} \frac{\Omega_+\left(\frac{i}{a_1}\right)}{J_+\left(\frac{i}{a_1}\right)} \frac{(3-4\nu)^{1/2} l_1^{i\varepsilon} a^{1/2-i\varepsilon}}{2G\gamma(\frac{1}{2}+i\varepsilon)}. \tag{128}$$

Splitting $T(q)$ into a product of analytic functions we find $T(q) = T_+ T_-$ with

$$T_+(q) = \frac{2\pi G}{4(1-\nu)} \frac{2^{-2q}\gamma(2q+3)}{\gamma(q-i\varepsilon+\frac{3}{2})\gamma(q+i\varepsilon+\frac{3}{2})}, \tag{129}$$

$$T_-(q) = \frac{-2^{2q+2}\gamma(-2q-2)}{\gamma(i\varepsilon-q-\frac{1}{2})\gamma(-q-i\varepsilon-\frac{1}{2})}. \tag{130}$$

Then, as in Atkinson (1982b), the functional equation (126) can be rearranged as the following functional equation:

$$T_-(q)G(q) + (T_-(q) - T_-(i\varepsilon-\tfrac{1}{2}))\frac{E^*}{2(q+\frac{3}{2}-i\varepsilon)} + \frac{E}{2(q+\frac{3}{2}+i\varepsilon)}(T_-(q) - T_-(-i\varepsilon-\tfrac{1}{2}))$$
$$= \frac{-F_+}{T_+} - \frac{E^*}{2(q+\frac{3}{2}-i\varepsilon)} T_-(i\varepsilon-\tfrac{1}{2}) - \frac{E}{2(q+\frac{3}{2}+i\varepsilon)} T_-(-i\varepsilon-\tfrac{1}{2}) = I(q). \tag{131}$$

The asymptotic properties of $T_\pm$ can be used together with Liouville's theorem to deduce that $I(q) = 0$.

From Atkinson (1982a) the stresses ahead of the fracture can be evaluated from the Mellin transform

$$M(R^2(\bar{T}_{R\theta} + i\bar{T}_{\theta\theta}))|_{\theta=0} = \frac{4(1-\nu)e^{iq\pi}}{(1+(3-4\nu)e^{2iq\pi})} i\bar{F}_+(q), \tag{132}$$

and the stress in the contact zone from (124). Hence we can deduce on $\theta = \pi$, $R \ll 1$

$$\bar{T}_{\theta\theta} = -\frac{(1-2\nu)}{2(1-\nu)} \frac{\Omega_+\left(\frac{i}{a_1}\right)}{s} \left(\frac{a}{R}\right)^{1/2} \Re\left(\frac{i(\tau_1+i\tau_2)}{J_+\left(\frac{i}{a_1}\right)\gamma(\frac{1}{2}+i\varepsilon)} \left(\frac{l_1}{4a}\right)^{i\varepsilon}\right). \tag{133}$$

Similarly we can deduce a result [cf. (2.26) of Atkinson (1982b) from (132)] for the stresses on $\theta = 0$ from which it would initially appear that the stresses are still oscillatory. However, from (107), the oscillatory parts cancel out. If we now consider the stress in the contact zone (133) we have to determine the length over which it remains compressive and, for the Comninou model, for which $\bar{T}_{\theta\theta}$ is bounded at $R = 1$. We can translate these results into the notation of Atkinson (1982b) by taking

$$P = \Im\left(\frac{a^{1/2-i\varepsilon}\Omega_-\left(\frac{i}{a_1}\right)(i\tau_1-\tau_2)}{\gamma(\frac{3}{2}+i\varepsilon)sJ_-\left(\frac{i}{a_1}\right)}\right), \quad Q = \Re\left(\frac{a^{1/2-i\varepsilon}\Omega_-\left(\frac{i}{a_1}\right)(i\tau_1-\tau_2)}{\gamma(\frac{3}{2}+i\varepsilon)sJ_+\left(\frac{i}{a_1}\right)}\right). \tag{134}$$

then the condition becomes

$$\left(\frac{P}{2}-\varepsilon Q\right)\cos\left(\varepsilon\log\frac{4a}{l_1}\right)+\left(\frac{Q}{2}+\varepsilon P\right)\sin\left(\varepsilon\log\frac{4a}{l_1}\right)=0. \tag{135}$$

It is clear from this that there are an infinity of contact zones lengths, however only one will satisfy the subsidiary condition that the stress be compressive along the contact zone. The above is then solved by

$$\cos\left(\varepsilon\log\frac{4a}{l_1}\right) = -\left(\frac{Q}{2}+\varepsilon P\right)\Big/(Q^2+P^2)^{1/2}(\varepsilon^2+\tfrac{1}{4})^{1/2}, \tag{136}$$

$$\sin\left(\varepsilon\log\frac{4a}{l_1}\right) = \left(\frac{P}{2}-\varepsilon Q\right)\Big/(Q^2+P^2)^{1/2}(\varepsilon^2+\tfrac{1}{4})^{1/2}. \tag{137}$$

In the case of pure tension, i.e. $\tau_2 = 0$, from the previous sections, it is clear that for small times the diffusion process induces a shear component, this has the effect of lengthening the contact zone. As in the elastic case the above relations can be used with the results from Atkinson (1982a,b) to show that the energy release rate for this model is identical to that obtained by considering the case with the oscillatory singularity as in Section 5.

The above matched asymptotic expansions are more accurate provided the contact zone length is small, for this we require that the contact zone is due to the interpenetration effect and not due to a purely shear loading. A shear loading acts to close the crack the contact zones are due to the loading, and the contact zone length may then be large. Hence our results above are valid, by analogy with Atkinson (1982b), when $P > Q$ this is true in the case of pure tension.

Due to the shear component induced by diffusion we can expect a larger contact zone length to be induced. We can see this from the above, taking $\nu = 0.2$ and $\nu_u = 0.4$ we plot l_1/a as a function of the non-dimensional time scale t' in Fig. 7. The complex gamma function is evaluated numerically using an algorithm described in Lanczos (1964). From this we see that initially the contact zone size is large. This then monotonically reduces to a standard elastic result.

In the impermeable case, the asymptotic behaviour of the pore pressure is that $\bar{P} \sim l_1^{1/2}p_0(s)$ and hence to leading order this does not affect the above analysis, so we can deduce that

$$\bar{T}_{\theta\theta} = -\frac{(1-2\nu)}{(1-\nu)}\frac{\bar{\Omega}_+\left(\frac{i}{a_1}\right)}{s}\left(\frac{a}{R}\right)^{1/2}\Re\left(\frac{i(\tau_1+i\tau_2)}{\bar{J}_+\left(\frac{i}{a_1}\right)\gamma(\frac{1}{2}+i\varepsilon)}\left(\frac{l_1}{4a}\right)^{i\varepsilon}\right). \tag{138}$$

7. STEADILY PROPAGATING FRACTURE

As in earlier papers by Craster and Atkinson (1992) and Atkinson and Craster (1991) the problem of steadily propagating fracture can be considered. This problem is considerably simpler as the explicit time dependence is removed. If the crack propagates at a steady velocity V then the field variables have the dependence on x, y, t $g = g(x-Vt, y)$ with g

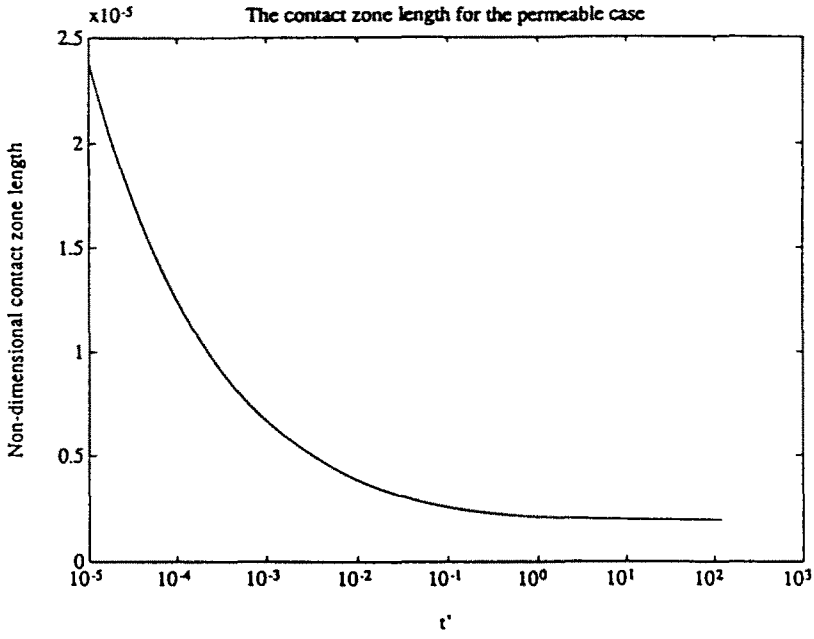

Fig. 7. Graph of the non-dimensional contact zone length l_1/a as a function of t' in the permeable interface case for $\nu = 0.2$, $\nu_u = 0.4$.

representing any field variable, i.e. we consider a steadily translating coordinate system. Hence the explicit time dependence is removed as $\partial/\partial t = -V(\partial/\partial x)$. The potential equations (30) and (31) become

$$\nabla^2\Psi = 0, \qquad c\nabla^4\Phi = -V\frac{\partial\nabla^2\Phi}{\partial x}. \tag{139, 140}$$

We can remove the explicit velocity dependence by adopting the following scaling

$$X = \frac{V}{c}x, \quad Y = \frac{V}{c}y, \quad U_i(X, Y) = \frac{V}{c}u_i(x, y), \tag{141}$$

$$\Phi(x, y) = \frac{c^2}{V^2}\Phi'(X, Y), \quad \Psi(x, y) = \frac{c^2}{V^2}\Psi'(X, Y), \tag{142}$$

and leaving the other field variables unchanged. For the interfacial problem, a similar analysis to that performed above can be repeated. The details of this we shall omit here and merely quote the results. We take a stress loading similar to that adopted in the impulsive case which now moves with the crack and decays as $X \to -\infty$, i.e.

$$\sigma_{YY} + i\sigma_{XY} = -(\tau_1 + i\tau_2)e^{X/a_1}, \tag{143}$$

where $a_1 = aV/c$ is a non-dimensional length scale. If the boundary is permeable the complex stress intensity factor as in (75) is

$$K^{(p)}(V) = \frac{\chi_+\left(\frac{i}{a_1}\right)}{i\omega_+\left(\frac{i}{a_1}\right)\Omega_0} K_e, \tag{144}$$

and if it is impermeable

$$K^{(im)}(V) = \frac{\bar{\chi}_+\left(\frac{i}{a_1}\right)}{i\bar{\omega}_+\left(\frac{i}{a_1}\right)\Omega_0} K_e, \tag{145}$$

with the elastic result (with drained parameters) as

$$K_e = \frac{(2\pi)^{1/2}(\tau_1 + i\tau_2)a^{(1/2 - i\varepsilon)}}{\gamma(\frac{1}{2} + i\varepsilon)}. \tag{146}$$

The functions χ, $\bar{\chi}$, ω, $\bar{\omega}$ and Ω_0 are defined in Appendix 1. Briefly, the oscillatory behaviour is unchanged and the complex power depends on the drained Poisson's ratio as in (76). The velocity dependent stress intensity scaling functions e.g.

$$\frac{\bar{\chi}_+\left(\frac{i}{a_1}\right)}{i\bar{\omega}_+\left(\frac{i}{a_1}\right)\Omega_0}$$

are plotted against a_1 for $\nu = 0.3$, $\nu_u = 0.4$ in Figs 8–10. It is interesting to note how the stress intensity factors alter for large a_1; in this limit the dominant behaviour comes from $\omega_+(i/a_1)$ and $\bar{\omega}_+(i/a_1)$. The real and imaginary parts behave as if the material is elastic for small values of a_1, and then the effect of the fluid diffusion becomes significant. It is also

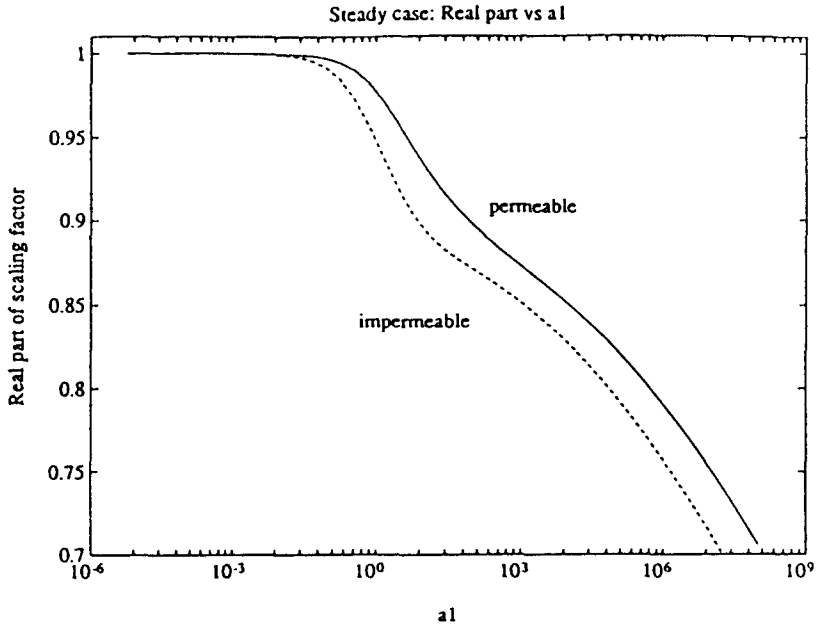

Fig. 8. The real part of the complex scaling factor versus a_1 for $\nu = 0.2$, $\nu_u = 0.4$.

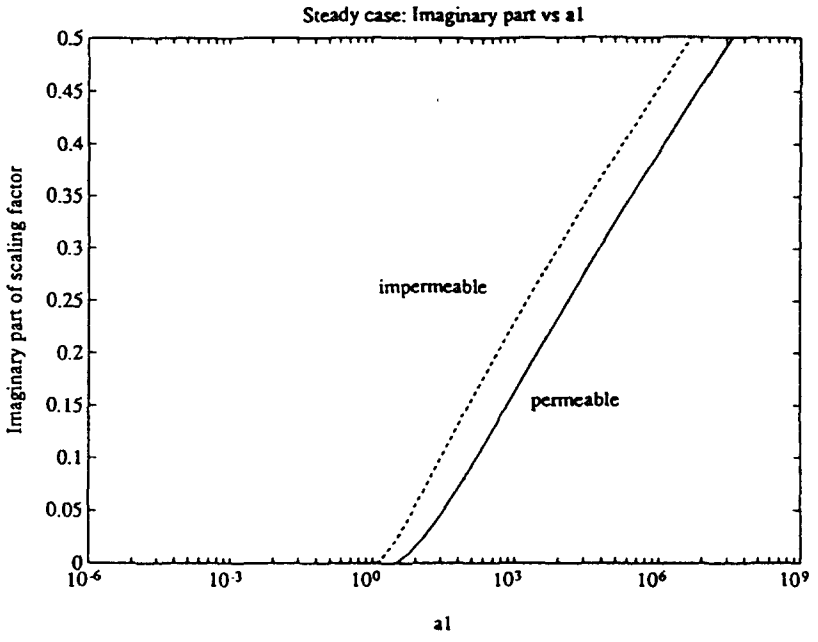

Fig. 9. The imaginary part of the complex scaling factor versus a_1 for $\nu = 0.2$, $\nu_u = 0.4$.

interesting to note that the modulus of the scaling function tends to a constant. Numerically it appears (see Fig. 8) that

$$\left|\frac{\chi_+(i0)}{i\Omega_0\omega_+(i0)}\right| \to \left(\frac{(1-\nu)(3-4\nu_u)}{(3-4\nu)(1-\nu_u)}\right)\left(\frac{\cosh(\pi\varepsilon_u)}{\cosh(\pi\varepsilon)}\right). \tag{147}$$

In particular this implies,

$$|K^{(p)}(V)| \to \left(\frac{(1-\nu)(3-4\nu_u)}{(3-4\nu)(1-\nu_u)}\right)\left(\frac{\cosh(\pi\varepsilon_u)}{\cosh(\pi\varepsilon)}\right)^{1/2}|K_e|, \tag{148}$$

with K_e now the elastic stress intensity factor with undrained coefficients, in terms of the

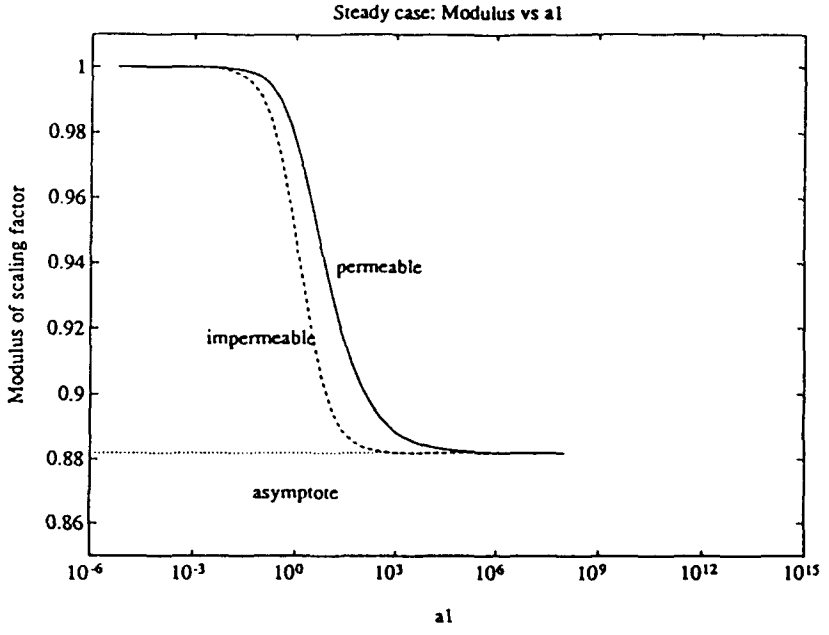

Fig. 10. The imaginary part of the complex scaling factor versus a_1 for $\nu = 0.2$, $\nu_u = 0.4$.

matching type arguments in Appendix E of Craster and Atkinson (1992) and the stress intensity factor for the undrained outer material. There is an identical result for the impermeable case. This is the square of the result predicted by the energy release rate argument used in Section 5 for the impulsive cases. The limit of large a_1 corresponds to large velocities (where dynamic effects may alter the results) or to cases where the consolidation coefficient is small, e.g. clays. This limit is reminiscent of the steady cases considered in Craster and Atkinson (1992) and Atkinson and Craster (1991) where the infinite velocity limit of the steady stress intensity factors was the square of the result predicted using the energy release rate. In the steady case this was rationalized by Rice and Simons (1976) using a heuristic argument based on comparing the near tip displacement fields in the drained and undrained cases. Such a heuristic argument does not appear to work here, although the result that (147) is the square of the result predicted by the energy release rate, as in the previous steady cases, does suggest that this is always the case. We can find no way to conclusively prove this.

For comparison with previous results we consider the energy release rate for a steadily propagating shear crack on an impermeable plane in an otherwise homogeneous material and compare this with the energy release rate for a steadily propagating crack on an impermeable interface. From Craster and Atkinson (1992) we take the mode 2 stress intensity factor $K_{II}(V)$ for the semi-infinite impermeable crack† in a homogeneous medium subjected to a moving shear loading $\sigma_{XY} = -|\tau|\, e^{X a_1}$, with $\tau = \tau_1 + i\tau_2$, then

$$K_{II}(V) = \frac{\sqrt{2}|\tau|a^{1/2}(\bar{\eta} - \frac{1}{2})\left(1 + \dfrac{1}{a_1}\right)^{1/2}}{\left(\left(\bar{\eta} - \dfrac{1}{a_1}\right)\left(1 + \dfrac{1}{a_1}\right)^{1/2} + \dfrac{1}{a_1^{1/2}}\right)}. \tag{149}$$

The energy release rate‡, the energy required per unit advance of the crack, is given (in the region $y > 0$) by

$$\bar{G}(V) = \frac{K_{II}^2(V)(1-\nu)}{4G}. \tag{150}$$

We plot $\bar{G}(V)$ divided by the energy release rate for an identically loaded elastic solid [replace $K_{II}(V)$ by $\sqrt{2}|\tau|a^{1/2}$ in (150)] as curve d in Fig. 11 for $\nu = 0.12$, $\nu_u = 0.31$.

In the (impermeable) interfacial case

$$\bar{G}^{(im)}(V) = \frac{|K^{(im)}(V)|^2(3-4\nu)}{16G(1-\nu)}. \tag{151}$$

With $K^{(im)}(V)$ as defined in (145) above, we plot the energy release rate for

$$\frac{4G\bar{G}^{(im)}(V)}{2|(\tau_1 + i\tau_2)|^2 a(1-\nu)}, \tag{152}$$

i.e. comparing the interfacial energy release rate against the equivalently loaded elastic material, in Fig. 11 as curve c for the same Poisson's ratios as in the homogeneous case above. The flow of energy, for small a_1, into the crack tip is less for the interface case, suggesting that the velocity of propagation will be smaller for this debonding; for larger a_1

† We note that this stress intensity factor is the same as that for the shear fracture on and impermeable plane in an undamaged homogeneous material and for mode I (tensile) fracture where the crack faces are impermeable, it appears that for steadily propagating fracture in homogeneous materials there are only two different stress intensity factors depending upon the pore pressure boundary conditions, i.e. permeable or impermeable, on the crack faces.

‡ The authors apologize for the notation, here G is the shear modulus and $\bar{G}(V)$ is the energy release rate.

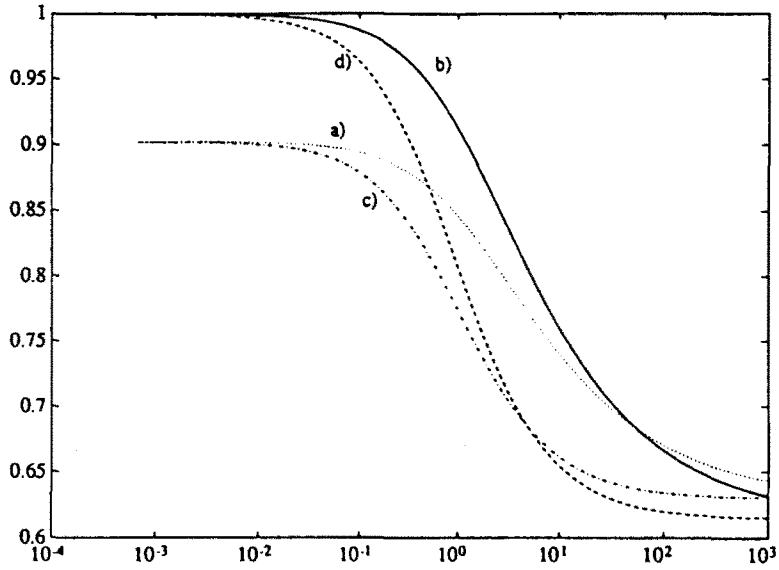

Fig. 11. The energy release rates (normalized as in the text) as functions of $a_1 = aV/c$ for Poisson's ratios $\nu = 0.12$, $\nu_u = 0.31$ the curves correspond to (a) the permeable interface, (b) permeable interface (homogeneous case), (c) the impermeable interface and (d) impermeable interface (homogeneous case).

this situation reverses. There is little difference between the various cases in this limit. The curves b, a in Fig. 11 are the equivalent normalized energy release rates for the permeable interfaces. As can be seen the permeable cases have higher values, the impermeable interface traps the fluid in the upper half plane leading to larger energy dissipation. The smaller energy release rates suggest that less energy is available for fracture, a similar result for the homogeneous cases is found in Rudnicki and Koutsibelas (1991). We note that as $\nu \to \nu_u \to \frac{1}{2}$ the interfacial and homogeneous energy release rates tend to each other. The X axis of Fig. 11 contains the range of a_1 thought to apply for fault creep events.

From the contact zone analysis of Section 6 we can deduce that for larger velocities we would expect a large contact zone, this may also help to retard the crack velocity if this is due to a large shear component. For the complex stress intensity factor, which is always inseparable into just tensile and shear components the inseparability becomes more marked. The large imaginary component will alter the phase of the complex stress intensity factor, although it is physically more interesting to consider the energy release rates as above. The diffusion of the fluid through the material induces stresses which have a large effect on the near crack tip fields. In the steadily propagating cases considered in Atkinson and Craster (1991) and Craster and Atkinson (1992) for homogeneous materials the analytical solutions showed a wake of pore pressure behind the crack tip it is the dissipation of energy caused by the diffusion process which tends to retard velocity of the fracture. The wake was more pronounced in the cases with impermeable crack faces as the fluid could not pass through the crack walls. It is clear from Figs 8–10 that the influence of diffusion is to induce a significant change in scaling factors.

7.1. *Crack tip fields*

In the case of steadily propagating fracture the pore pressure diffusion equation (17) becomes

$$\nabla^2 p = \frac{-V}{\kappa Q}\frac{\partial p}{\partial x} - \frac{\alpha V}{\kappa}\frac{\partial e}{\partial x}, \tag{153}$$

and the elastic Navier equation with the coupling term (16) remains unaltered. As in Atkinson and Craster (1991) and Craster and Atkinson (1992) we can deduce simple near

crack tip fields. To leading order the stresses are the classical elastic solution with velocity dependent stress intensity factors. The near crack tip pore pressure can be found from

$$\nabla^2 p = \frac{-\alpha V}{\kappa}\frac{\partial e}{\partial x}, \tag{154}$$

and an eigensolution of $\nabla^2 p = 0$ which together satisfy the appropriate pore pressure boundary condition.

In the permeable case we find that

$$p \sim \frac{-\alpha V(1-2\nu) r^{1/2} e^{\varepsilon(\theta-\pi)}}{4G\kappa(2\pi)^{1/2}\cosh(\pi\varepsilon)} \Re\left(r^{i\varepsilon} K^{(p)}(V)(e^{3i\theta/2} - e^{-i\theta/2})\right). \tag{155}$$

In the impermeable case

$$p \sim p_0 - \frac{\alpha V(1-2\nu) r^{1/2} e^{\varepsilon(\theta-\pi)}}{4G\kappa(2\pi)^{1/2}\cosh(\pi\varepsilon)} \Re\left(r^{i\varepsilon} K^{(\mathrm{im})}(V)\left(e^{3i\theta/2} + \frac{(\frac{1}{2}-i\varepsilon)}{(\frac{1}{2}+i\varepsilon)} e^{-i\theta/2}\right)\right). \tag{156}$$

In both cases the pore pressure is clearly oscillatory. This raises interesting experimental possibilities. It is often thought that the mathematically equivalent thermoelastic equations uncouple. This assumption is implicit in most of the work on fracture in thermoelastic materials, e.g. Kuo (1990). This could be checked, for instance using the experimental work of Zehnder and Rosakis (1991) on the temperature distribution of dynamically propagating cracks in steel. In the mode I tensile case (for a homogeneous material) that they consider, although performed at significantly larger velocities for which our theory here is necessarily valid (because of the neglect of inertia), the temperature contours are quantitatively similar to those in Atkinson and Craster (1991). The oscillatory behaviour for the pore pressure we have shown above is driven by the dilatation, and so will only be present if the equations are fully coupled. This would provide an interesting and conclusive test on the validity or otherwise of the uncoupling assumption.

So far in this paper we have not discussed problems in which the pore pressure conditions are mixed, i.e. permeable crack faces and interface ahead of the crack impermeable. The problem in the impulsive case is outlined in Appendix 4; we can, however, derive some asymptotic results for the near crack tip fields. As in the unmixed cases, the stresses will be the usual elastic solution with a velocity dependent stress intensity factor and the pore pressure will be given in the same manner as above, as

$$p \sim K_3(V) r^{1/2} \sin\frac{\theta}{2} - \frac{\alpha V(1-2\nu) r^{1/2} e^{-\varepsilon\pi}}{4G\kappa(2\pi)^{1/2}\cosh(\pi\varepsilon)} \Re\Bigg(r^{-i\varepsilon} e^{\varepsilon\theta} K^*(V)$$
$$\times \left(e^{-3i\theta/2} - e^{i\theta/2 - \varepsilon\pi}\frac{(((\frac{3}{4}-\varepsilon^2)+(\frac{1}{4}+\varepsilon^2)e^{2\pi\varepsilon})+2\varepsilon i)}{2(\frac{1}{4}+\varepsilon^2)\sinh(\pi\varepsilon)}\right) + \frac{e^{\varepsilon(\pi-\theta)} e^{i\theta/2} r^{i\varepsilon}(-\frac{1}{2}+i\varepsilon)K(V)}{(\frac{1}{4}+\varepsilon^2)\sinh(\pi\varepsilon)}\Bigg). \tag{157}$$

This first term is an eigensolution of $\nabla^2 p = 0$ and the second term a particular solution of (154). The coefficients $K_3(V)$ and $K(V) = K_1(V) + iK_2(V)$ would need to be deduced from the solution of a matrix Wiener–Hopf equation (see Appendix 4). We note that these solutions will also be the leading order solutions for the crack tip fields of an arbitrarily moving crack.

8. CONCLUSION

The problem of interfacial fracture between a linear diffusive elastic medium and a rigid substrate has been tackled analytically using the Wiener–Hopf technique. The complex time dependent stress intensity factors are evaluated in Laplace transform space and inverted

both analytically for small times and numerically for all times. This complex stress intensity factor characterizes the near crack tip stress fields. The main results are:

- The time dependent complex stress intensity factors for an impulsively loaded semi-infinite crack in the permeable (92) and impermeable (93) interface cases are deduced; the analytic results are given in Laplace transform space. These results are then inverted numerically and checked in the small time limit using a physical argument based on the energy release rate.
- The small time behaviour of the intensity factors, e.g. Figs 1–3 show that the diffusion can be expected to play an important role. For example, the complex stress intensity factor is multiplied by a time dependent factor which has a large imaginary component. The energy release rates for the two different interfaces are compared with the equivalent homogeneous cases.
- A contact zone analysis is performed using the methods outlined in Atkinson (1982a,b). The analysis assumes that the ratio of the contact zone length to the loading length is much smaller than unity, hence the results will not be so accurate for asymmetric problems. The effect of the pore pressure/temperature diffusion on the contact zone length is quantified.

The case of a steadily propagating, permeable or impermeable, semi-infinite interfacial fracture is also considered here:

- The velocity dependent complex stress intensity factors (144) and (145) are identified. For large velocities, or materials with small consolidation coefficients, the intensity factors are again significantly altered by the diffusion process, and it can be expected to play an important role. For example, the imaginary component of the velocity dependent factor which multiplies the stress intensity factor becomes large, which alters the character of the near crack tip stress fields. The energy release rates for the interfacial and the equivalently loaded homogeneous cases are plotted.
- Simple near crack tip pore pressure fields (155)–(157) are deduced which are oscillatory in character. The oscillations will only occur for the fully coupled equations. The result in (157) is deduced for the fully mixed problem, permeable crack faces and impermeable ahead, see Appendix 4. This could form the basis for experimental work to verify or otherwise the uncoupling of the thermoelastic equations.

The stress intensity factors as functions of $t' = tc/d^2$ (or in the steady cases of $a_1 = aV/c$) depend only on the material parameters ν, ν_u (the drained and undrained Poisson's ratios). The coupling plays an important role for all materials as either $t' \to 0$ (or $a_1 \to \infty$). As $\nu \to \nu_u$ the effect of the coupling decreases.

These analytic results are all derived using an idealised loading. However, it is possible to superimpose the loadings to represent more general situations. These analytic results provide a basis upon which future analytical, numerical and experimental studies can be based.

Acknowledgements—The authors would like to thank S. Appleby of Schlumberger Cambridge Research for her constructive criticism and subsequent improvement of the style and grammar of the manuscript.

C. Atkinson would like to thank the Royal Society/SERC Industrial Fellowship scheme for their support and R. Craster the SERC for a Research Studentship.

The computing and other facilities of Schlumberger Cambridge Research are gratefully acknowledged.

REFERENCES

Abramowitz, M. and Stegun, I. A. (1970). *Handbook of Mathematical Functions*. Dover, New York.

Aravas, N. and Sharma, S. M. (1991). An elastoplastic analysis of the interface crack with contact zones. *J. Mech. Phys. Solids* **39**, 311–344.

Atkinson, C. (1977a). On stress singularities and interfaces in linear elastic fracture mechanics. *Int. J. Fracture* **13**, 807–820.

Atkinson, C. (1977b). Dynamic crack problems in dissimilar media. In *Mechanics of Fracture* 4: *Elastodynamic Crack Problems* (Edited by G. C. Sih), pp. 213–248. Leyden, Noordhoff.

Atkinson, C. (1982a). The interface crack with a contact zone (an analytical treatment). *Int. J. Fracture* **18**, 161–177.

Atkinson, C. (1982b). The interface crack with a contact zone (the crack of finite length). *Int. J. Fracture* **19**, 131–138.

Atkinson, C. and Craster, R. V. (1991). Plane strain fracture in poroelastic media. *Proc. R. Soc. Lond. A* **434**, 605–633.
Atkinson, C. and Craster, R. V. (1992). The application of invariant integrals in diffusive elastic solids. *Phil. Trans. R. Soc.* (accepted).
Atkinson, C. and Leppington, F. G. (1983). The asymptotic solution of some integral equations. *IMA J. Appl. Math.* **31**, 169–182.
Biot, M. A. (1941). General theory of three-dimensional consolidation. *J. Appl. Phys.* **12**, 155–164.
Biot, M. A. (1955). Thermoelasticity and irreversible thermodynamics. *J. Appl. Phys.* **27**, 240–253.
Biot, M. A. (1956). General solutions of the equations of elasticity and consolidation for a porous material. *ASME J. Appl. Mech.* **78**, 91–96.
Boley, B. A. and Wiener, J. H. (1960). *Theory of Thermal Stresses*. Wiley, New York.
Champion, C. R. and Atkinson, C. (1991). A crack at the interface between two power-law materials under plane strain loading. *Proc. R. Soc. Lond. A* **432**, 547–553.
Craster, R. V. and Atkinson, C. (1991). Shear cracks in thermoelastic and Poroelastic media. *J. Mech. Phys. Solids* (accepted).
Drory, M. D., Thouless, M. D. and Evans, A. G. (1988). On the decohesion of residually stressed thin films. *Acta Metall.* **36**, 2019.
England, A. H. (1965). A crack between dissimilar media. *ASME J. Appl. Mech.* **32**, 400–402.
Gautesen, A. K. and Dundurs, J. (1987). The interface crack in a tension field. *ASME J. Appl. Mech.* **54**, 93–98.
Gautesen, A. K. and Dundurs, J. (1988). The interface crack under combined loading. *ASME J. Appl. Mech.* **55**, 580–586.
Green, J. S. (1955). The calculation of the time responses of linear systems. Ph.D. Thesis, Department of Mathematics, Imperial College, London.
Hein, V. L. and Erdogan, F. (1971). Stress singularities in a two-material wedge. *Int. J. Fract. Mech.* **7**, 317–330.
Kuo, A. (1990). Interface crack between two dissimilar half spaces subjected to a uniform heat flow at infinity—open crack. *ASME J. Appl. Mech.* **57**, 359–364.
Lanczos, C. (1964). A precise approximation of the gamma function. *SIAM J. Num. Anal.* **1**, 86–96.
Malyshev, B. M. and Salganik, R. L. (1965). The strength of adhesive joints using the theory of the crack. *Int. J. Fract. Mech.* **1**, 114–128.
McNamee, J. and Gibson, R. E. (1960). Displacement functions and linear transforms applied to diffusion through porous elastic media. *Q. J. Mech. Appl. Math.* **13**, 98.
Muskhelishvili, N. I. (1953). *Some Basic Problems of the Mathematical Theory of Elasticity*. Noordhoff, Groningen, Holland.
Ni, L. and Nemat-Nasser, S. (1991). Interface cracks in anisotropic dissimilar materials: an analytic solution. *J. Mech. Phys. Solids* **39**(1), 113–144.
Noble, B. (1958). *Methods Based on the Wiener–Hopf Technique for the Solution of Partial differential Equations*. Pergamon Press, Oxford.
Qu, J. and Bassani, J. L. (1989). Cracks on bimaterial and bicrystal interfaces. *J. Mech. Phys. Solids* **37**, 418.
Rice, J. R. and Cleary, M. P. (1976). Some basic stress-diffusion solutions for fluid saturated elastic porous media with compressible constituents. *Rev. Geophys. Space Phys.* **14**, 227–241.
Rice, J. R. and Simons, D. A. (1976). The stabilisation of spreading shear faults by coupled deformation-diffusion effects in fluids-infiltrated porous materials. *J. Geophys. Res.* **81**(29), 5322–5334.
Rudnicki, J. W. and Koutsibelas, D. A. (1991). Steady propagation of plane strain shear cracks on an impermeable plane in an elastic diffusive solid. *Int. J. Solids Structures* **27**, 205.
Shield, R. T. (1982). Uniqueness for elastic crack and punch problems. *ASME J. Appl. Mech.* **49**, 516–518.
Skempton, A. (1954). The pore pressure coefficients A and B. *Geotechnique* **4**, 143–147.
Stehfest, H. (1970). Numerical inversion of Laplace transforms. *CACM* **13**, 47–49 and 624.
Talbot, A. (1979). The accurate numerical inversion of Laplace transforms. *J. Inst. Maths Applics* **23**, 97–120.
Verruijt, A. (1969). The completeness of Biot's solution of the coupled thermoelastic problem. *Q. Appl. Math.* **26**, 485.
Williams, M. L. (1959). The stresses around a fault or crack in dissimilar media. *Bull. Seismol. Soc. America* **49**, 199–204.
Willis, J. R. (1972). The penny shaped crack on an interface. *Q. J. Mech. Appl. Math.* **25**, 367.
Yang, W., Suo, Z. and Shih, C. F. (1991). Mechanics of dynamic debonding. *Proc. R. Soc. Lond. A* **433**, 679–697.
Zehnder, A. T. and Rosakis, A. J. (1991). On the temperature distribution at the vicinity of dynamically propagating cracks in 4340 steel. *J. Mech. Phys. Solids* **39**, 385–415.

APPENDIX 1: PRODUCT SPLITS

We split the function $W(\xi)$, appearing in (69), following the analysis in some detail and then briefly outline the main results for the other functions in the text.

To perform the product split for $W(\xi)$, defined as

$$W(\xi) = \frac{|\xi|}{\xi} - \left(\frac{1}{2\eta_u} + \frac{1}{2\bar{\eta}(1-\nu_u)} (\Gamma|\xi| - \xi^2) \right). \tag{A1}$$

we note that $W(\xi)$ has no zeros in the cut plane. Then for convenience we consider the function $J(\xi)$ where

$$J(\xi) = \frac{\xi_-^m}{\xi_+^m}\left(1 - \frac{\xi}{|\xi|}\left(\frac{1}{2\eta_u} + \frac{(\Gamma|\xi| - \xi^2)}{2\tilde{\eta}(1-\nu_u)}\right)\right). \tag{A2}$$

then as

$$\xi \to +\infty, \quad J(\xi) \to \frac{1}{2(1-\nu)} = J_0 \quad \text{and as} \quad \xi \to -\infty, \quad J(\xi) \to e^{-2\pi i m}\frac{(3-4\nu)}{2(1-\nu)}.$$

To perform the product split for $J(\xi) = J_+(\xi)J_-(\xi)$ and then deduce W_+ and W_-, we consider

$$\log\left(\frac{J(\xi)}{J_0}\right) = \log J_+ + \log\left(\frac{J_-}{J_0}\right). \tag{A3}$$

Implicit in this splitting procedure, is, that for the convergence of the contour integrals (A5), $J(\xi)$ must tend to J_0 as $|\xi| \to \infty$. Therefore we deduce that

$$m = \frac{1}{2\pi i}\log(3-4\nu). \tag{A4}$$

The usual Cauchy representations for a product split are

$$\pm\frac{1}{2\pi i}\int_{-\infty \pm id}^{+\infty \pm id} \frac{\log\left(\frac{J(z)}{J_0}\right)}{z-\xi}\,dz = \begin{cases} \log J_+(\xi) \\ \log\left(\frac{J_-(\xi)}{J_0}\right). \end{cases} \tag{A5}$$

with d real and positive, d then tends to zero. The function $\log(J(\xi)/J_0)$ has branch cuts from $i0_+$ to $i\infty$ and from $i0_-$ to $-i\infty$ which can be checked numerically by following $\log(J(\xi)/J_0)$ along either side of the imaginary axis, i.e. $\xi = 0_\pm + yi$ for $-\infty \leqslant y \leqslant \infty$.

As $J(\xi)/J_0 \to 1 + O(1/\xi^2)$ when $|\xi| \to \infty$ the contribution to the integral from closing the contour of integration about an arc at infinity is zero. Defining

$$z = \frac{\left(1 - \frac{1}{2\eta_u}\left(1 + \frac{\eta_u}{\tilde{\eta}(1-\nu_u)}(y^2 - iy(1-y^2)^{1/2})\right)\right)}{\left(1 + \frac{1}{2\eta_u}\left(1 + \frac{\eta_u}{\tilde{\eta}(1-\nu_u)}(y^2 + iy(1-y^2)^{1/2})\right)\right)}, \tag{A6}$$

θ to be the argument of z, and z_2 as

$$z_2 = \frac{\left(1 - \left(\frac{1}{2\eta_u} + \frac{y^2 - y(y^2-1)^{1/2}}{2\tilde{\eta}(1-\nu_u)}\right)\right)}{\left(1 + \left(\frac{1}{2\eta_u} + \frac{y^2 - y(y^2-1)^{1/2}}{2\tilde{\eta}(1-\nu_u)}\right)\right)}, \tag{A7}$$

we collapse the path of integration about the branch cut in the upper half plane to give:

$$\log\left(\frac{J_-(\xi)}{J_0}\right) = \frac{-1}{2\pi i}\left(\int_0^1 \frac{\log((3-4\nu)z^*)}{(y+i\xi)}dy + \int_1^\infty \frac{\log((3-4\nu)z_2)}{(y+i\xi)}dy\right), \tag{A8}$$

the * denoting the complex conjugate, and although initially defined in the lower half plane, is by analytic continuation a function valid in the whole complex plane except for the branch cut from $i0_+$ to $i\infty$.

Similarly J_+ can be evaluated by collapsing the integral around the lower branch cut

$$\log J_+(\xi) = \frac{1}{2\pi i}\left(\int_0^1 \frac{\log((3-4\nu)z)}{(y-i\xi)}dy + \int_1^\infty \frac{\log((3-4\nu)z_2)}{(y-i\xi)}dy\right), \tag{A9}$$

although initially defined in the upper half plane the function can be analytically continued to define a function valid everywhere except for the branch cut from $i0_-$ to $-i\infty$. Using (A9 and A8) we can therefore deduce that

$$J(\xi) = J_0\exp\left(\frac{1}{\pi}\left(\log(3-4\nu)\tan^{-1}\left(\frac{1}{\xi}\right) + \int_0^1 (\xi\log|z| + y\theta)\frac{dy}{(y^2+\xi^2)}\right)\right) + J_0\exp\left(\frac{1}{\pi}\int_1^\infty \frac{\xi\log((3-4\nu)z_2)}{(y^2+\xi^2)}dy\right). \tag{A10}$$

This can now be checked numerically with (A2) for real ξ.

As $\xi \to 0_+$ then $J_-/J_0 \to J_+^*$ therefore we can deduce that

$$|J_+(0_+)| = \left(\frac{1-\nu}{1-\nu_u}\right)^{1/2}, \qquad |J_-(0_-)| = \left(\frac{(1-\nu)(3-4\nu_u)}{(1-\nu_u)(3-4\nu)}\right)^{1/2}, \tag{A11}$$

which are useful checks on (A9).

In the limit as $\delta \to 0$ the integrals can be rescaled and it can be shown that

$$J_+(\delta) = \left(\frac{1-\nu}{1-\nu_u}\right)^{1/2} \exp\left(\frac{i}{4\pi}\log\left(1+\frac{1}{\delta^2}\right)\log\left(\frac{3-4\nu}{3-4\nu_u}\right)\right). \tag{A12}$$

with a similar expression for $J_-(\delta)$. This oscillatory behaviour as δ tends to 0 makes the evaluation of the inverse Laplace transform (92) a difficult process. Hence

$$W_- = \frac{J_-}{\xi_-^{1/2+m}} \quad \text{and} \quad W_+ = J_+ \xi_+^{1/2+m}.$$

Note that in the elastic limit when $\nu \to \nu_u$, or equivalently $\bar{\eta} \to \infty$, we have the result that

$$W(\xi) = J_0 \frac{\xi_+^{m+1/2}}{\xi_-^{m+1/2}}.$$

This substitution then leads to the classical interfacial results.

Defining $\bar{W}(\xi)$, from (86), as

$$\bar{W}(\xi) = \frac{|\xi|}{\xi} - \frac{1}{2\eta_u} + \frac{\xi^2(|\xi|-\Gamma)}{2\Gamma\bar{\eta}(1-\nu_u)}, \tag{A13}$$

we follow the analysis above closely to define $J(\xi)$ as

$$J(\xi) = \frac{\xi_-^m}{\xi_+^m}\left(1 - \frac{\xi}{2\eta_u|\xi|} + \frac{\xi(\xi^2-|\xi|\Gamma)}{2\bar{\eta}(1-\nu_u)\Gamma}\right). \tag{A14}$$

m can be deduced to be given as before by (A4). The main difference from the previous product split is that $J(\xi)$ has a zero at $\pm i\beta + 0$, (i.e. on the imaginary axis approached from the right) with

$$\beta = \left(\frac{\bar{\eta}(2-\bar{\eta}) + \bar{\eta}(\bar{\eta}^2+4\bar{\eta})^{1/2}}{2(2\bar{\eta}-1)}\right)^{1/2}. \tag{A15}$$

As $|\beta| \geqslant 1$, the logarithm of $J(iy)/J_0$ is undefined for $1 \leqslant |y| \leqslant \beta$. The branch cuts go from $i0_+$ to $\pm i\infty$ which can be checked numerically. Taking

$$z = \left(\frac{1 - \dfrac{1}{2\eta_u} + \dfrac{y^2}{2\bar{\eta}(1-\nu_u)} + \dfrac{iy^3}{2\bar{\eta}(1-\nu_u)(1-y^2)^{1/2}}}{1 + \dfrac{1}{2\eta_u} - \dfrac{y^2}{2\bar{\eta}(1-\nu_u)} + \dfrac{iy^3}{2\bar{\eta}(1-\nu_u)(1-y^2)^{1/2}}}\right), \tag{A16}$$

and

$$z_2 = \left(\frac{1 - \dfrac{1}{2\eta_u} + \dfrac{y(-y^2+y(y^2-1)^{1/2})}{2\bar{\eta}(1-\nu_u)(y^2-1)^{1/2}}}{1 + \dfrac{1}{2\eta_u} - \dfrac{y(-y^2+y(y^2-1)^{1/2})}{2\bar{\eta}(1-\nu_u)(y^2-1)^{1/2}}}\right), \tag{A17}$$

the main results are

$$\log J_+(\xi) = \frac{1}{2\pi i}\left(\int_0^1 \frac{\log((3-4\nu)z)}{(y-i\xi)}dy + \int_1^\infty \frac{\log((3-4\nu)|z_2|)}{(y-i\xi)}dy\right) + \tfrac{1}{2}\log\left(\frac{\beta-i\xi}{1-i\xi}\right). \tag{A18}$$

$$J(\xi) = J_0\left(\frac{\beta^2+\xi^2}{1+\xi^2}\right)^{1/2} \exp\frac{1}{\pi}\left(\log(3-4\nu)\tan^{-1}\left(\frac{1}{\xi}\right) + \int_0^1 (\xi\log|z| + y\theta)\frac{dy}{(y^2+\xi^2)} + \int_1^\infty \frac{\xi\log(3-4\nu)|z_2|\,dy}{(y^2+\xi^2)}\right). \tag{A19}$$

Also $W_- = \dfrac{J_-}{\xi_-^{(m+1/2)}}$, $W_+ = J_+\xi_+^{(m+1/2)}$ and $|J_+(0_+)| = |J_-(0_-)|$.

The product split of $\Omega(\xi)$ into a product of functions analytic in the "upper", and "lower" half complex ξ

planes respectively, is similar to the factorization of the function $N(\xi)$ performed in Appendix 1 of Atkinson and Craster (1991). As a result the factorization is only sketched briefly here. Recalling that

$$\Omega(\xi) = \xi^2 - (\Gamma|\xi| + (3-4\nu_u)\tilde{\eta}). \tag{A20}$$

This function has branch cuts from $\pm i0_+$ to $\pm i$ and can be shown to have no zeros in the cut plane. The functions Ω_+, Ω_- are defined in the usual manner by similar Cauchy representations to (A5) with Ω replacing J. Asymptotically as

$$|\xi| \to \infty, \quad \Omega(\xi) \to -\left(\frac{(3-4\nu)(1-\nu_u)}{2(\nu_u-\nu)}\right) = -\tfrac{1}{2}(1+2\tilde{\eta}(3-4\nu_u)) = -\Omega_0.$$

In particular by collapsing the contour integrals around the branch cuts we can deduce that

$$\log(\Omega_+(\xi)) = \frac{-1}{\pi}\int_0^1 \tan^{-1}\left(\frac{p(1-p^2)^{1/2}}{p^2+(3-4\nu_u)\tilde{\eta}}\right)\frac{dp}{(p-i\xi)}, \tag{A21}$$

$$\Omega_+(0) = \left(\frac{(3-4\nu_u)(1-\nu)}{(3-4\nu)(1-\nu_u)}\right)^{1/2}, \tag{A22}$$

which is checked numerically against (178) and

$$\Omega(\xi) = -\Omega_0 \exp\left(-\frac{1}{\pi}\int_0^1 \tan^{-1}\left(\frac{p(1-p^2)^{1/2}}{p^2+(3-4\nu_u)\tilde{\eta}}\right)\frac{2p\,dp}{(p^2+\xi^2)}\right). \tag{A23}$$

which is checked numerically against (A20) using the general purpose NAG integration routine D01AJF. The results are accurate to machine accuracy. The product split of $\bar{\Omega}(\xi)$ is related to that of $\bar{N}(\xi)$ in Craster and Atkinson (1992) letting

$$\bar{\Omega}(\xi) = \xi^2 - \frac{|\xi|\xi^2}{\Gamma} + (3-4\nu_u)\tilde{\eta}, \tag{A24}$$

we can deduce that $\bar{\Omega}(\xi)$ [unlike $\bar{N}(\xi)$] has no zeros in the cut plane, therefore

$$\log(\bar{\Omega}_+(\xi)) = \frac{1}{\pi}\int_0^1 \tan^{-1}\left(\frac{p^3}{(1-p^2)^{1/2}(p^2-(3-4\nu_u)\tilde{\eta})}\right)\frac{dp}{(p-i\xi)}, \tag{A25}$$

$\bar{\Omega}_+(0) = \Omega_+(0)$ and

$$\bar{\Omega}(\xi) = \Omega_0 \exp\left(\frac{1}{\pi}\int_0^1 \tan^{-1}\left(\frac{p^3}{(1-p^2)^{1/2}(p^2-(3-4\nu_u)\tilde{\eta})}\right)\frac{2p\,dp}{(p^2+\xi^2)}\right), \tag{A26}$$

which can be verified numerically. In the steadily propagating case the functions which arise can be split in a similar manner and the results are just quoted here. Note that in the steady case $\Gamma^2 = \xi^2 + i\xi$.

$$\chi_+(\xi) = \xi_+^{1/2}\Gamma_+ - \xi + i\tilde{\eta}(3-4\nu_u), \qquad \bar{\chi}_+(\xi) = \xi - \frac{\xi\xi_+^{1/2}}{\Gamma_+} + i\tilde{\eta}(3-4\nu_u), \tag{A27, A28}$$

$$\omega(\xi) = \frac{\xi^m}{\xi_+^m} - \left(1 - \frac{|\xi|}{2\eta_u\xi} + \frac{(|\xi|-\Gamma)}{2i\tilde{\eta}(1-\nu_u)}\right), \tag{A29}$$

$$\log\omega_+(\xi) = \frac{1}{2\pi i}\int_0^1 \log\left(\frac{(3-4\nu)\left(1-\dfrac{1}{2\eta_u}-\dfrac{(iy+y^{1/2}(1-y)^{1/2})}{2i\tilde{\eta}(1-\nu_u)}\right)}{1+\dfrac{1}{2\eta_u}+\dfrac{(iy-y^{1/2}(1-y)^{1/2})}{2i\tilde{\eta}(1-\nu_u)}}\right)\frac{dy}{y-i\xi}$$

$$+\frac{1}{2\pi i}\int_1^\infty \log\left(\frac{(3-4\nu)\left(1-\dfrac{1}{2\eta_u}-\dfrac{(y-y^{1/2}(y-1)^{1/2})}{2\tilde{\eta}(1-\nu_u)}\right)}{1+\dfrac{1}{\eta_u}+\dfrac{(y-y^{1/2}(y-1)^{1/2})}{2\tilde{\eta}(1-\nu_u)}}\right)\frac{dy}{y-i\xi}, \tag{A30}$$

$$\bar{\omega}(\xi) = \frac{\xi^m}{\xi_+^m}\left(1 - \frac{|\xi|}{2\eta_u\xi} + \frac{(\xi^2-\Gamma|\xi|)}{2i\Gamma\tilde{\eta}(1-\nu_u)}\right), \tag{A31}$$

which has a zero at $-i\beta+0_+$ with

$$\beta = \bar{\eta}\left(\frac{(2-\bar{\eta})+(\bar{\eta}^2+4\bar{\eta})^{1/2}}{2(2\bar{\eta}-1)}\right). \tag{A32}$$

$$\log\bar{\omega}_+(\xi) = \tfrac{1}{2}\log\left(\frac{\beta-i\xi}{1-i\xi}\right)+\frac{1}{2\pi i}\int_0^1 \log\left(\frac{(3-4\nu)\left(1-\frac{1}{2\eta_u}-\frac{y}{2\bar{\eta}(1-\nu_u)}+\frac{i(y-y^2)^{1/2}}{2\bar{\eta}(1-\nu_u)}\right)}{\left(1+\frac{1}{2\eta_u}+\frac{y}{2\bar{\eta}(1-\nu_u)}+\frac{i(y-y^2)^{1/2}}{2\bar{\eta}(1-\nu_u)}\right)}\right)\frac{dy}{y-i\xi}$$

$$+\frac{1}{2\pi i}\int_1^\infty \log\left|\frac{(3-4\nu)\left(1-\frac{1}{2\eta_u}+\frac{y^2-y(y^2+y)^{1/2}}{2\bar{\eta}(1-\nu_u)(y^2+y)^{1/2}}\right)}{1+\frac{1}{2\eta_u}-\frac{y^2-y(y^2+y)^{1/2}}{2\bar{\eta}(1-\nu_u)(y^2+y)^{1/2}}}\right|\frac{dy}{y-i\xi}. \tag{A33}$$

APPENDIX 2: FOURIER RESULTS

To evaluate the asymptotic behaviour of the stress fields we require the following Fourier inversion

$$f_+(x) = \frac{1}{2\pi}\int_{-\infty}^{+\infty}\frac{e^{-i\xi x}}{\xi_+^{n+1/2+iz}}\,d\xi. \tag{A34}$$

Recalling that the functions $\xi_+^{1/2+n+iz}$ have branch cuts from $i0_+$ to $+i\infty$ the integral is evaluated (for n integer and z real) by collapsing this integral around the branch cut from $i0_-$ to $-i\infty$. The result $\gamma(z)\gamma(1-z) = \pi\,\mathrm{cosec}\,(\pi z)$ is also required to give the following Tauberian result

$$f_+(x) = \frac{e^{\pi z/2}x^{n+iz-1/2}H(x)}{i^{n+1/2}\gamma(n+iz+\frac{1}{2})}, \tag{A35}$$

and $\gamma(z)$, the Gamma function, is defined in the usual manner to be

$$\gamma(z+1) = \int_0^\infty t^z e^{-t}\,dt. \tag{A36}$$

Also to invert the minus transforms we have $f_-(-x) = f_+^*(x)$, i.e. the complex conjugate of the equivalent plus transform.

APPENDIX 3

The Fourier transformed displacements, stresses and pore pressure:

$$U_1 = -i\xi(A_1 e^{-|\xi|Y}+A_2 e^{-\Gamma Y}+YB_1 e^{-|\xi|Y}), \tag{A37}$$

$$U_2 = -|\xi|A_1 e^{-|\xi|Y}-\Gamma A_2 e^{-\Gamma Y}-YB_1|\xi|e^{-|\xi|Y}-(3-4\nu_u)B_1 e^{-|\xi|Y}, \tag{A38}$$

$$P = \frac{2G\eta}{\alpha}(\Gamma^2-\xi^2)A_2 e^{-\Gamma Y}-2\alpha Q(1-2\nu_u)|\xi|B_1 e^{-|\xi|Y}, \tag{A39}$$

$$T_{12} = 2Gi\xi(A_1|\xi|e^{-|\xi|Y}+\Gamma A_2 e^{-\Gamma Y}+Y|\xi|B_1 e^{-|\xi|Y}+(1-2\nu_u)B_1 e^{-|\xi|Y}), \tag{A40}$$

$$T_{22} = 2G(\xi^2(A_1 e^{-|\xi|Y}+A_2 e^{-\Gamma Y})+2(1-\nu_u)|\xi|B_1 e^{-|\xi|Y}+Y\xi^2 B_1 e^{-|\xi|Y}), \tag{A41}$$

$$T_{11} = 2G(-Y\xi^2 B_1 e^{-|\xi|Y}-(\xi^2 A_1 e^{-|\xi|Y}+\Gamma^2 A_2 e^{-\Gamma Y})+2\nu_u|\xi|B_1 e^{-|\xi|Y}). \tag{A42}$$

APPENDIX 4: THE FULLY MIXED PROBLEM

In previous papers Atkinson and Craster (1991) and Craster and Atkinson (1992), the problems of fracture in undamaged continuous materials are considered. In particular the situation of mixed pore pressure boundary conditions is investigated, e.g. in the tensile case consider a permeable crack; the symmetry of the problem then sets an impermeable condition on the fracture plane ahead of the crack. In the interfacial situation we could similarly consider a crack with permeable crack faces with the interface ahead of the crack impermeable. Let us briefly consider the impulsive case *cf.* Section 3.1 and in addition to (55)–(58) define the following half range transforms;

$$P_+ = \int_0^\infty P(X,0,s)\,e^{i\xi X}\,dX, \qquad R_- = \int_{-\infty}^0 \frac{\partial P(X,0,s)}{\partial Y} e^{i\xi Y}\,dX, \tag{A43, A44}$$

and use the same loadings as in Section 3.1. The resulting matrix Wiener–Hopf equation is

$$\begin{pmatrix} T_+ \\ \tau_+ \end{pmatrix} - \begin{pmatrix} \dfrac{\tau_1 a_1 c^{1/2}}{s^{3/2}(1+i\xi a_1)} \\ \dfrac{\tau_2 a_1 c^{1/2}}{s^{3/2}(1+i\xi a_1)} \end{pmatrix} + \frac{3}{2B(1+\nu_u)} \begin{pmatrix} 2(1-\nu_u)P_+ \\ \dfrac{-i(1-2\nu_u)R_-}{\xi} \end{pmatrix}$$

$$= \frac{2G\xi}{\Gamma i\bar{\Omega}(\xi)} \begin{pmatrix} -2\bar{\eta}i\xi(1-\nu_u) & -\overline{Z(\xi)} \\ Z(\xi) & \dfrac{-2i\Gamma|\xi|(1-\nu_u)\bar{\eta}}{\xi} \end{pmatrix} \begin{pmatrix} V_- + \dfrac{(3-4\nu_u)3R_-}{4GB(1+\nu_u)\xi^2} \\ U_- \end{pmatrix}. \tag{A45}$$

$\bar{\Omega}$ and $Z(\xi)$ are defined as in (A24), (68) and

$$\overline{Z(\xi)} = \xi^2(\Gamma - |\xi|) + \Gamma\bar{\eta}(3-4\nu_u) - 2\bar{\eta}|\xi|(1-\nu_u). \tag{A46}$$

The added complication of the mixed pore pressure boundary conditions introduces an asymmetry in the matrix equations which we, so far, have been unable to factorize.

APPENDIX 5: NUMERICAL INVERSION OF LAPLACE TRANSFORMS

In the previous works by the authors we have used the Stehfest (1970) algorithm to invert Laplace transforms numerically. This algorithm has proved to be both fast and accurate, but suffers from numerical rounding errors which can corrupt the results. The algorithm is not suitable for inverting functions which are complex and have unusual behaviour at particular points. In our case the function $J_+(i/a_1)$ is a function which is discontinuous at the origin as it is approached from 0_+. In this case a better algorithm is that of Talbot (1979) which is in essence based on the earlier thesis of Green (1955). The algorithm has to be slightly adapted for use here. In Talbot's paper the Bromwich inversion contour is replaced by a substitute contour, L, with $\Re(s) \to -\infty$ at each end. This avoids complications, from the oscillations of e^{st}, which would arise in the direct numerical integration along the Bromwich contour. This substitute contour clearly has to enclose all the singularities and branch cuts of the function to be inverted, so limits the range of application of the method, i.e. functions with an infinite number of singularities with imaginary parts tending to infinity could not be inverted, but the method is sufficiently general to invert most functions usually encountered.

The notation used here will follow Talbot very closely and the adaptation required will be briefly sketched. Taking the function to be inverted as $F(s)$ we can introduce a scaling λ and shift σ parameter which are used to ensure that L contains all the singularities. Then we invert $F(\lambda s+\sigma)$:

$$f(t) = \frac{\lambda e^{\sigma t}}{2\pi i} \int_L e^{\lambda s t} F(\lambda s+\sigma)\,ds. \tag{A47}$$

Now Talbot maps the interval $-2\pi i$ to $2\pi i$ onto a path, M, described by an analytic function

$$s = S(z) = \frac{z}{2}\left(\coth\frac{z}{2} + \nu\right),$$

with ν a free parameter, so that

$$f(t) = \frac{1}{2\pi i}\int_M Q(z)\,dz = \frac{1}{2\pi i}\int_{-2\pi}^{2\pi} Q(iy)\,dy, \tag{A48}$$

with $Q(z) = \lambda\, e^{t(\lambda S+\sigma)} F(\lambda S+\sigma)S'(z)$. Talbot then assumes that $Q(-iy) = Q^*(iy)$. This is true if $F(s)$ is real, however, $J_+(i/a_1)$ in the text is complex so we follow Talbot by defining

$$\theta_k = \frac{k\pi}{n}, \quad \alpha = \theta\cot\theta, \quad S(z) = \alpha + i\nu\theta, \quad \beta = \theta + \alpha(\alpha-1)\theta, \tag{A49}$$

$$S'(z) = \tfrac{1}{2}(\nu + i\beta), \quad F(\lambda s+\sigma) = G_1 + iH_1, \quad F((\lambda s+\sigma)^*) = G_2 + iH_2, \tag{A50}$$

then approximate the integral (A47) with the trapezoidal rule and take a suitable choice of σ, λ, ν and n. $f(t)$ becomes

$$f(t) = \frac{\lambda e^{\sigma t}}{2n} \sum_{k=0}^{2n-1}{}' e^{\pi i k/n} (((vG_1 - \beta H_1) + (vG_2 + \beta H_2)) \cos(v\theta t)$$
$$+ ((vH_2 - \beta G_2) - (\beta G_1 + vH_1)) \sin(v\theta t) + i((\beta G_1 + vH_1) + (-\beta G_2 + vH_2)) \cos(v\theta t)$$
$$+ i((vG_1 - \beta H_1) - (vG_2 + \beta H_2)) \sin(v\theta t))|_{\theta = \theta_k}. \quad \text{(A51)}$$

The prime on the summation is used to denote that we take half the values in the sum when k takes the values 0 and $n-1$. The error in this algorithm is discussed in some detail by Talbot and a similar analysis will hold here.